UNIVERSIDADE D
COIMBRA

João Afonso Dourado Santos Silva

EVALUATION OF WIND SIMULATION MODELS USING A CLIMATOLOGY APPROACH

Dissertação no âmbito do Mestrado Integrado em Engenharia Mecânica na Especialidade de Energia e Ambiente, orientada pelo Professor Doutor António Manuel Gameiro Lopes e Doutor Omar Herrera Sanchez (menzio GmbH) e apresentada ao Departamento de Engenharia Mecânica, da Faculdade de Ciências e Tecnologia da Universidade de Coimbra.

Outubro de 2020

Evaluation of wind simulation models using a climatology approach

Submitted in Partial Fulfilment of the Requirements for the Degree of Master in Mechanical Engineering in the speciality of Energy and Environment

Avaliação de modelos de simulação de vento usando uma abordagem climatológica

Author

João Afonso Dourado Santos Silva

Advisors

António Manuel Gameiro Lopes, PhD.

Omar Herrera Sanchez (menzio GmbH), PhD.

Jury

President	**Pedro de Figueiredo Vieira Carvalheira, PhD.** **Professor, University of Coimbra**
Vowel	**Almerindo Domingues Ferreira, PhD.** **Professor, University of Coimbra**
Advisor	**António Manuel Gameiro Lopes, PhD.** **Professor, University of Coimbra**

Institutional Collaboration

Universidade de Coimbra

menzio GmbH

Coimbra, October 2020

ACKNOWLEDGEMENTS

First, I would like to give special thanks to my advisor, Professor Antonio Gameiro, for having provided the opportunity to learn and work on an exciting topic. Also, I would like to thank him and my co-advisor, Professor Omar Herrera Sanchez, for their guidance and counselling, and for always being available to help.

I want to thank IPMA, CIM Coimbra and CIM Viseu for contributing with indispensable data for carrying out this study.

I want to thank all my friends that were present during my academic life. Also, I am immensely grateful for my friends that motivated me during the 2020 pandemic and the writing of the thesis.

Finally, I would like to thank my family for always being present, on the good and bad moments, and for believing in me.

Abstract

The ability to predict the wind's behaviour through computer applications, CFD, is fundamental to the development of the energy sector and to the prevention of environmental hazards. Although there are models that predict the wind's behaviour reliably, flows around complex topographies remain a challenge.

The main objective of this work is to evaluate the performance of the numerical models implemented in the software WindStation when applied to complex terrain. The evaluation was performed by comparing the numeric results with the measured wind data using a climatology approach. The wind data was provided by meteorological stations from IPMA, CIM Coimbra, and CIM Viseu in the central region of Portugal, and was measured at 10 meters high.

Discrepancies between the predicted results and the measured data were significant. These disparities can be a consequence of the use of a large calculation domain and subsequent inability to refine the mesh properly, and of the absence of measurements at higher altitudes. The latter was confirmed with the improvement of the results when including wind data from a meteorological station located near the top of a mountain.

Keywords: Wind, Complex terrain, Climatology, CFD, WindStation.

Resumo

A capacidade de prever o comportamento do vento através de aplicações de computador, CFD, é fundamental para o desenvolvimento do setor energético e para a prevenção de riscos ambientais. Embora existam modelos que preveem o comportamento do vento de forma confiável, fluxos em torno de topografias complexas permanecem um desafio.

O objetivo principal deste trabalho é avaliar o desempenho dos modelos numéricos implementados no software WindStation quando aplicados em terrenos complexos. A avaliação foi realizada comparando os resultados numéricos com os dados das medições do vento usando uma abordagem climatológica. Os dados de vento foram fornecidos pelas estações meteorológicas do IPMA, CIM Coimbra e CIM Viseu na região centro de Portugal e foram medidos a 10 metros de altura.

As discrepâncias entre os resultados previstos e os dados das medições foram significativas. Estas discrepâncias pode ser um resultado da utilização de um grande domínio de cálculo e consequente incapacidade de refinar adequadamente a malha, e à falta de medições em altitudes mais elevadas. Este último foi confirmado com uma melhoria dos resultados ao incluir dados de vento de uma estação meteorológica localizada perto do topo de uma montanha.

Palavras-chave: Vento, Terreno complexo, Climatologia, CFD, WindStation.

Contents

LIST OF FIGURES

LIST OF TABLES

LIST OF SYMBOLS AND ACRONYMS/ ABBREVIATIONS

List of Symbols

A, k – Weibull parameters

c_p – Specific heat capacity [J.kg.K^{-1}]

C_μ – Turbulence model constant

f – Frequency [%]

g – Gravitational acceleration [m.s^{-2}]

k – Turbulence kinetic energy [m^2.s^{-2}]

L_d – Dissipation length scale

p – Pressure [N.m^{-2}]

P – Wind power density [W.m^{-2}]

Pr – Laminar Prandtl number

R_{conv} – Maximum residual value

R_k, R_m, R_u, R_v, R_w, R_ε, R_θ – Calculated residual values

S_{ci} – Coriolis forces source term

S_{ui} – Porosity source term

T – Local temperature [K]

T_I – Flow turbulence intensity

u – Wind speed [m.s^{-1}]

u_i – Generic Cartesian velocity component [m.s^{-1}]

U – Mean wind speed [m.s^{-1}]

V, U –Velocity [m.s^{-1}]

x_i – Generic Cartesian coordinate [m]

β – Thermal expansion coefficient [K^{-1}]

Γ – Generic diffusion coefficient

ε – Dissipation rate of turbulence kinetic energy [m^2.s^{-3}]

θ – Potential temperature [K]

θ_{ref} – Reference potential temperature [K]

μ – Laminar dynamic viscosity [N.s.m^{-2}]

μ_{eff} – Effective dynamic viscosity [N.s.m^{-2}]

μ_t – Turbulent dynamic viscosity [N.s.m^{-2}]

ρ – Fluid density [kg.m^{-3}]

σ_θ – Turbulent Prandtl number

ϕ – Generic variable

Acronyms/Abbreviations

CFD – Computational Fluid Dynamics

CIM – *Comunidade Intermunicipal*

DFreq – Wind direction frequency

HighRes – High resolution

IPMA – *Instituto Português do Mar e da Atmosfera*

LowRes – Low resolution

MO – Monin-Obukhov

WSpd – Mean wind speed

1. INTRODUCTION

Since the early days, the wind has been very influential in the development of humankind. It shapes the way we live, as we must adapt to climate conditions and natural disasters, such as wildfires, hurricanes, and storms. Besides changing our surroundings, the wind is also harnessed for our benefit, providing natural ventilation, facilitating transportation, creating energy for water pumps, irrigation, and food processing machines, and, more recently, it is being used as a renewable source of electrical energy.

With the industrialisation of countries and their increase in energy consumption, nations are becoming more concerned with the resulting environmental issues. Regarding these matters, countries are making efforts to shift their principal sources of energy from fossil fuels to renewable sources. During the year of 2019, wind energy was one of the most significant and expanding sources of energy. According to "Renewables 2020 Global Status Report" released by REN21 (2020), "Wind energy accounted for an estimated 57% of Denmark's electricity generation in 2019, with high shares also in Ireland (32%), Uruguay (29.5%), Portugal (26.4%) and several other countries. Capacity in operation worldwide at year's end was enough to provide an estimated 5.9% of global generation". This report also proclaims an increase of the wind energy generation throughout the years, as presented in Figure 1 and Figure 2 for the global capacity and the global offshore capacity, respectively.

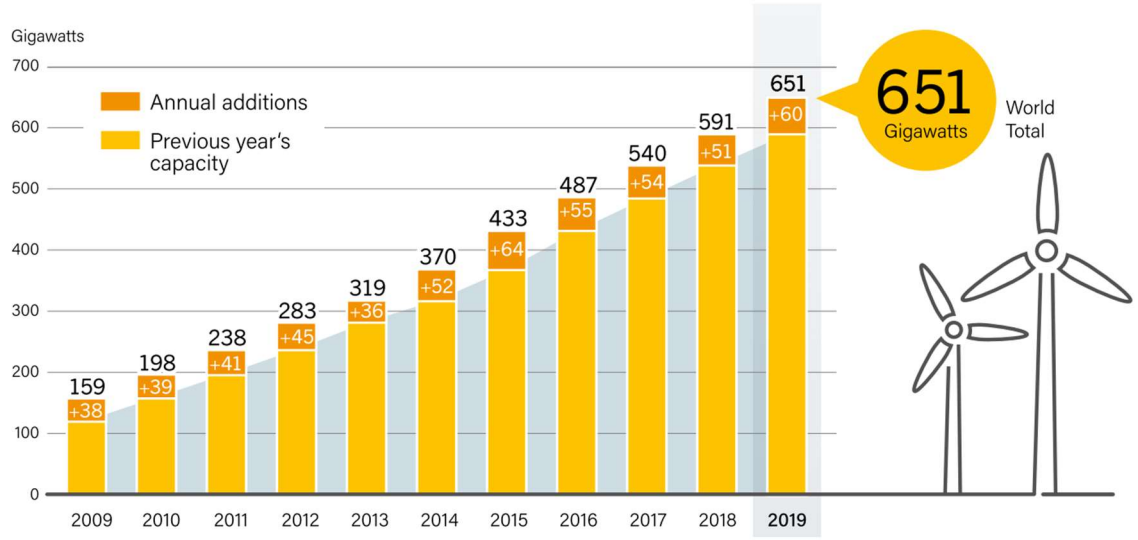

Figure 1 - Wind power global capacity from 2009 to 2019. Adapted from REN21 (2020).

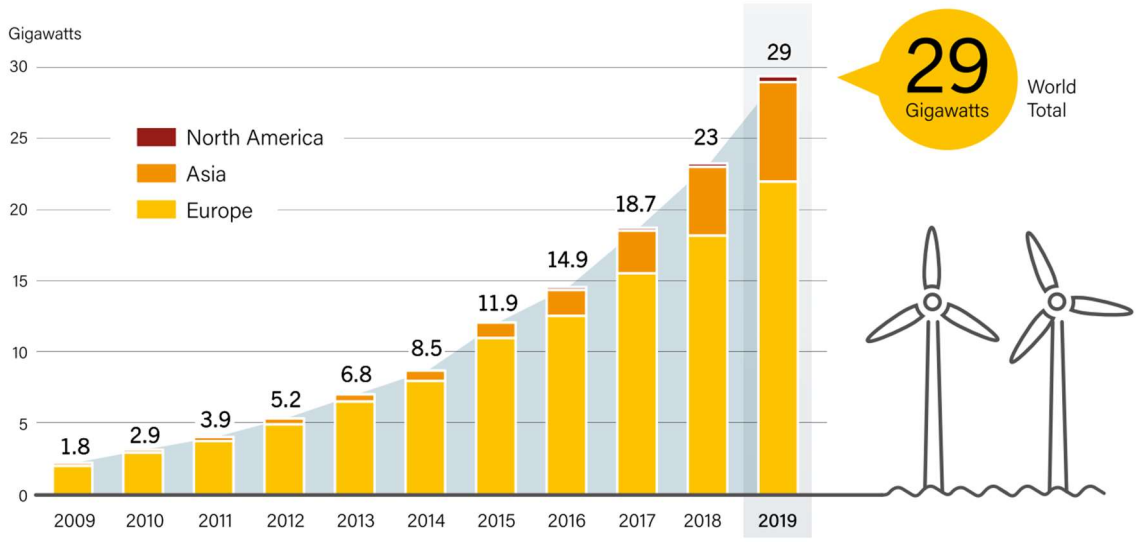

Figure 2 - Wind power global offshore capacity from 2009 to 2019. Adapted from REN21 (2020).

In recent years, technology has become more prevalent and essential for the functioning of society. Most of the working sectors operate based on computer applications, and the engineering industry is no exception. In the wind sector, computational tools provide a more efficient approach to study and predict wind behaviour. Furthermore, with the improvement of computing power, these tools, based on numeric calculations and artificial intelligence, are being further optimised to produce better results in less time. These tools can have various applications. They can be used to predict the behaviour of environmental issues, such as wildfires, storms, and hurricanes; analyse the wind's influence on skyscrapers, bridges, and other large structures; optimise the design of transports and other moving mechanisms; study and improve the efficiency of wind farms and wind-related sources of energy; and others.

Although there are diverse models that predict the wind's behaviour and provide reliable results, some flows, usually around complex geometries and topographies, remain a challenge. Therefore, they are used as validation studies for existing and developing models. Following this topic, the goal of this thesis is to evaluate the Computational Fluid Dynamics (CFD) software, WindStation (Lopes, 2020), when applied to complex topography with input data from meteorological stations. For the evaluation, wind measurements from the centre region of Portugal, provided by *Instituto Português do Mar e da Atmosfera* (IPMA), *Comunidade Intermunicipal de Coimbra* (CIM Coimbra), and *Comunidade Intermunicipal*

de Viseu (CIM Viseu), were used. These measurements were taken with a climatology approach to obtain a better representation of the wind characteristics in the study location.

WindStation is a wind analysis software that uses numerical simulations to assess wind resources in complex terrain. Additionally, it offers numerous tools that simplify and optimise the simulation process. For this type of study, WindStation processes the climatology statistics of the provided wind measurements and gives a prediction for the study location, also in statistics. To evaluate the software performance, the predicted results were compared to the remaining measurements of the study location. Mean wind speed and wind direction frequency were used as the values for the comparison method.

1.1. Thesis Overview

The present essay is divided into five parts: Introduction, Theoretical Background, Resolution Method, Results and Analysis, and Conclusions.

The current chapter, Introduction, presents the thesis' themes and goals, its structure, and a summary of the relevant literature researched by the author.

In Chapter 2, Theoretical Background, concepts and definitions that were deemed essential to the understanding of the thesis are introduced. Also, a summary of the WindStation's equations and functionalities is presented.

Chapter 3, Resolution Method, describes the input parameters, the methodology, and the tools used in this study. Furthermore, it describes the sensitivity analyses and the evaluation method that were utilised.

Chapter 4, Results and Analysis, presents the simulations results and their respective analysis, providing conclusive outcomes and their possible explanation.

Chapter 5, Conclusions, is a chapter dedicated to the overall summary of this dissertation, lessons learned from previous researches and their results, and possible developments and suggestions for future studies.

1.2. Literature Review

This section lists the researched literature that was considered relevant for this study. Some references are mentioned during this thesis to complement specific topics and practices. In chapter 2.2 and 2.3, most references are used to complement technicalities of the software WindStation, and thus, were not consulted by the author, with the exception of the User's Manual by Lopes (2020).

The first two mentioned studies resorted to the software WindStation. These were written in the same academic context and can be considered preceding work for this thesis.

The thesis of Jeanmonod (2015) presents a validation study of WindStation for the Askervein case and a case with complex topography in Serra da Lousã, Portugal. In both instances, a sensitivity analysis was made to verify which parameters had more impact on the results. The Askervein case was considered successful, and its sensitivity analysis demonstrated that the parameters variation had a low influence on the results. On the other hand, the complex topography case offered a greater challenge to validate, and its sensitivity analysis showed that the relation between the parameters and the results was more difficult to analyse.

Duarte (2018) presents a study of the software WindStation for the Bolund case and a wind farm case, in northern France. In both situations, the analysis was accomplished by verifying the prediction of the wind behaviour on assigned locations and comparing them to their respective measurements, considering an initial fixed wind velocity. The study of the Bolund case demonstrated that in instances with small topographic domains, certain variation parameters, such as turbulence and advection models, are not significant for the results; and that in terrain sections with more complex geometries the model has difficulty to provide accurate results. In the wind farm case, a dependency between the input location and the results location was proven.

The thesis of Teneler (2011) studies the performance of the software WindSim, which is a CFD tool based on a nonlinear flow model for predicting wind energy production on a wind farm, located in Northern Sweden. The wind farm is situated in complex terrain, and its study used wind statistics data with a yearly time frame. For the analysis, the WindSim results were compared with the results estimated by WAsP and with measurements. This study concluded that both the WindSim and WAsP simulation

overestimate the wind speed and energy production. Additionally, in this case, using a forest canopy model provides more accurate results.

Wallbank (2008) presents a validation study of the software WindSim in complex terrain. Similar to the previously mentioned thesis, this study used wind statistics data, and its results were compared with results estimated by WasP. This study is composed of a sensitivity analysis and a full test. The sensitivity analysis showed that the parameters variation had a low impact on the results, except for the use of the forest feature that increased the error discrepancies. Additionally, this study verified that, when using the nesting feature, the more refined mesh was not more accurate. To conclude, the full test verified that both WindSim and WasP behaved similarly for the presented cases.

The following studies, although not as influential as the previous, helped to complement the current topic, providing information on shortcomings and setting expectations for this study. As an overview, most of the CFD's results were not satisfactory, and the height and quality of the wind measurements, the quality of the terrain information and obstacles, and the thermal influences were the main subjects referred as accountable when not adequately defined.

Berge et al. (2006), evaluates the performance of WindSim, 3DWind, and WasP in simulations on a wind farm with complex terrain in western Norway. This study uses two masts at 50 meters and one at 10 meters high, and analyses the mean absolute error, the vertical variations of wind speed and turbulence, and mesoscale wind variations across the wind farm. It concludes that there were no improvements when using the two CFD models, WindSim and 3DWind, when compared with a WasP model.

Cattin et al. (2006) is a study for WindSim on complex terrain in the region of the European Alps. This study compares the WindSim predictions to SODAR measurements and reveals discrepancies between both. The paper refers to recommendations and issues that might create the discrepancies.

Theodoropoulos and Deligiorgis (2009) is a validation study also for complex terrain in western Greece. This study uses a WindSim model, with RANs equations, to generate cross-predictions of climatology data from 7 masts. The predictions are then compared with the observations and a conventional WAsP model. This study concludes that, in cases with lack of high-altitude measurements or lack of terrain information, such as

induced thermal effects and or terrain imperfections, the CFD model cannot outperform the conventional WasP model.

2. THEORETICAL BACKGROUND

2.1. Wind

On the earth's atmosphere, the wind consists of a large-scale movement of air. This movement is caused by variations in atmospheric pressure originated by thermal differences and occurs from higher to lower pressures. It can also be caused by Coriolis forces, produced by the earth's rotation. Although the wind's nature is considered unpredictable, it has some recurrent behaviours that facilitate its study.

Wind profile. The wind profile represents the relation between wind speed and height. The terrain characteristics has a notable influence on the wind speed variation between different heights. Due to the friction with the earth's surface, the wind speed increases with the increase in height. Furthermore, the higher the terrain's roughness, the larger the discrepancy between low-altitude wind speeds and high-altitude wind speeds. Figure 3 represents the effect of roughness changes on the wind profile.

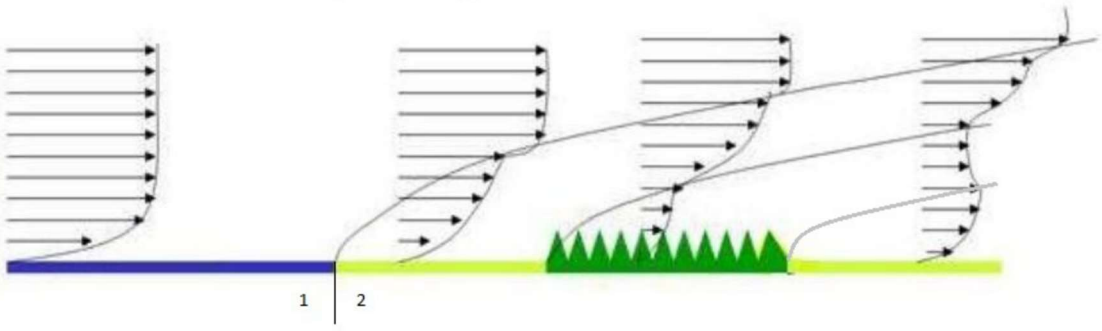

Figure 3 - Variation of the wind profile due to roughness changes. Adapted from Nilsson (2010).

Wind shear. The wind shear is referred to changes in wind speed and direction over relatively short distances due to weather conditions and terrain characteristics.

Atmospheric boundary layer. The atmospheric boundary layer is a lower part of the atmosphere where its contact with the earth's surface directly influences the wind behaviour. Due to its location, this layer is more prone to temperature changes by the surface heating, and it is also highly affected by the terrain's elevation and roughness, creating more turbulence. These factors make this layer unpredictable and a target of research.

Free atmosphere. Above the atmospheric boundary layer, the wind becomes almost independent of the earth's surface. In this zone, the wind's behaviour becomes mainly subjected to the balance between pressure forces and Coriolis forces.

Coriolis effect. The Coriolis effect represents a fictitious force used for simplifying calculus involving rotating systems. It depicts a force of inertia that, simultaneously with the drag and centrifugal force, acts on a rotating body, and is perpendicular to the plane defined by the axis of rotation and the velocity vector. This effect is present on the earth's surface and atmosphere, being influential on the dynamics of oceans and atmosphere and ballistic trajectories. Figure 4 represents the effect of the Coriolis forces on the wind in the north and south hemispheres.

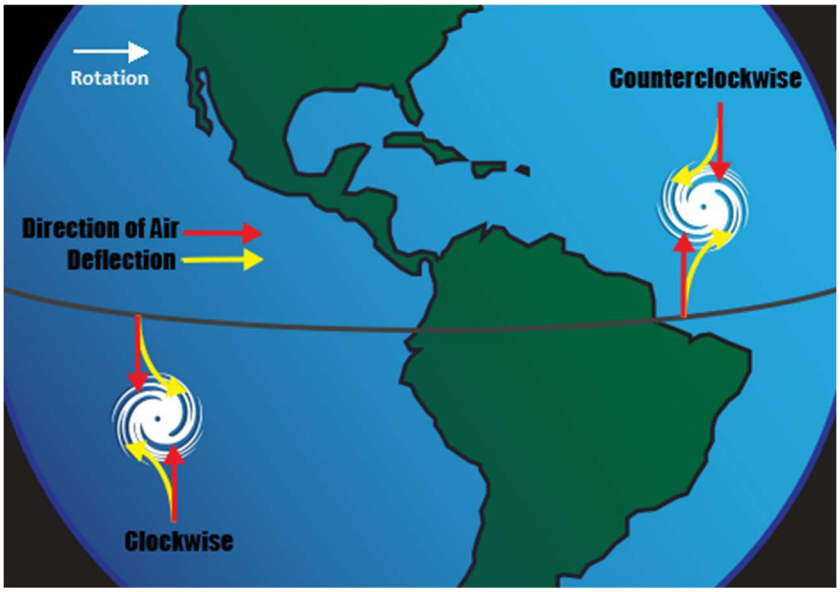

Figure 4 - Representation of the Coriolis effect on the wind in the earth's atmosphere. Adapted from NOAA SciJinks, "https://scijinks.gov/coriolis/".

2.2. WindStation as a CFD Tool

Computational Fluid Dynamics (CFD) is a branch of fluid mechanics that, recurring to digital computers, uses numeric analysis based on physical phenomena and conservation laws (conservation of mass, momentum, and energy) to produce quantitative predictions of fluid flows. With the current development in computing power, this subject becomes more relevant as it allows for a more suitable and cheaper method of predicting fluid flows. However, due to discretisation issues and turbulence modelling, CFD's predictions are never completely exact.

WindStation is a wind analysis software that uses numerical simulations to analyse turbulent flow over complex topography. It uses various input data such as terrain description, wind observations, and atmospheric stability, to create detailed problems and produce realistic predictions. For the numerical simulations, the software is based on the Navier-Stokes equations, continuity equation, and energy equation. Furthermore, it can make use of four different turbulence models, Coriolis forces, and a forest model.

This chapter gives an overview of the equations used for the numerical analysis. A more in-depth description of the equations is provided in the User's Manual by Lopes (2020).

2.2.1. Navier-Stokes Equations

The Navier-Stokes equations represent the conservation of momentum for fluid flows. Its steady-state formulation is:

$$\frac{\partial}{\partial x_j}\left(\rho u_i u_j\right) = -\frac{\partial p}{\partial x_i} + \frac{\partial}{\partial x_j}\left[\Gamma\left(2\frac{\partial u_j}{\partial x_j} - \frac{2}{3}div\vec{V}\right)\right] + \frac{\partial}{\partial x_j}\left[\Gamma\left(2\frac{\partial u_i}{\partial x_j} + \frac{\partial u_j}{\partial x_i}\right)\right] + \left(\rho g \beta\left(\theta - \theta_{ref}\right)\right)_{i=3} + S_{ci} + S_{ui} \tag{2.1}$$

where the term ρ [kg.m^{-3}] stands for the fluid density, x_i [m] is a generic Cartesian coordinate, u_i [m.s^{-1}] is a generic Cartesian velocity component, and p [N.m^{-2}] is pressure. $\Gamma = \mu_{eff} = \mu + \mu_t$ [N.s.m^{-2}] characterises the diffusion coefficient for momentum, where μ_{eff} [N.s.m^{-2}] is the effective dynamic viscosity, μ [N.s.m^{-2}] is the laminar dynamic viscosity, and μ_t [N.s.m^{-2}] is the turbulent dynamic viscosity.

In the buoyancy term, θ [K] is the potential temperature, corresponding to the adiabatic vertical temperature gradient, θ_{ref} [K] is the reference potential temperature, g

[m.s^{-2}] represents the gravitational acceleration, and $\beta = T^{-1}$ is the thermal expansion coefficient, with T [K] as the local temperature.

The term S_{ci} includes the Coriolis forces, caused by the earth's rotation. The term S_{ui} is used in the presence of porous obstacles and is computed with a forest model.

2.2.2. The Continuity Equation

The continuity equation establishes that, on an isolated system, there is mass conservation when a fluid moves from one point to another. This equation is represented by:

$$\frac{\partial(\rho u_i)}{\partial x_i} = 0 \tag{2.2}$$

2.2.3. The Energy Equation

The energy equation is written taking the potential temperature as the dependent variable:

$$\frac{\partial}{\partial x}\left(\rho c_p u\theta\right) + \frac{\partial}{\partial z}\left(\rho c_p w\theta\right) = \frac{\partial}{\partial x}\left(\Gamma\frac{\partial\theta}{\partial x}\right) + \frac{\partial}{\partial z}\left(\Gamma\frac{\partial\theta}{\partial z}\right) \tag{2.3}$$

For the case of a fluid domain, the diffusion coefficient, Γ, is:

$$\Gamma = \left(\frac{\mu}{Pr} + \frac{\mu_t}{\sigma_\theta}\right)c_p \tag{2.4}$$

where Pr represents the laminar Prandtl number, and σ_θ represents the turbulent Prandtl number, which depends on the adopted turbulence model. c_p [J.kg.K^{-1}] is the specific heat capacity.

2.2.4. Turbulence Modelling

WindStation has implemented four variants of the k-ε turbulence model. These models compute the turbulent viscosity making use of the transport equations, which are described in detail for each model in Lopes (2020). The available models are the following:

Standard k-ε model is the most versatile and used turbulence model (Launder & Spalding, 1972, 1974; Djilali et al., 1989). In this model, the turbulent viscosity is given by:

$$\mu_t = C_\mu \frac{\rho k^2}{\varepsilon} \tag{2.5}$$

where C_μ represents a turbulence model constant. The variable k [$m^2.s^{-2}$] is the turbulence kinetic energy and is a measure of the flow turbulence intensity, T_I, represented in eq. (2.6). The variable ε [$m^2.s^{-3}$] is the dissipation rate of turbulence kinetic energy, related to the dissipation length scale, L_d, represented in eq. (2.7).

$$T_I = \frac{\sqrt{\frac{2}{3}k}}{V} \Longrightarrow k = \frac{3}{2}(T_I V)^2 \tag{2.6}$$

$$L_d = {C_\mu}^{3/4}\frac{k^{3/4}}{\varepsilon} \Longrightarrow \varepsilon = {C_\mu}^{3/4}\frac{k^{3/4}}{L_d} \tag{2.7}$$

RNG k-ε model, which is more accurate when simulating rapidly strained flows, due to an additional term in the dissipation equation.

Realisable k-ε model, which was developed to obtain better results of simulations with boundary layer separation, rotating flows, and flows with strong streamline curvature.

Limited-length k-ε model, implemented mostly based on the proposal of Koblitz et al. (2013), it aims to solve a problem where the k-ε model tends to over predict the length scale, leading to large values of turbulent viscosity and overestimating the layer height. All the models allow the use of the Coriolis forces, being its use mandatory in the Limited-length k-ε model.

2.2.5. Numerical Solution

In the numerical simulation, the transport equations are transformed from their original Cartesian form into a generalised coordinate using the chain rule (Lopes et al., 1995). Following this transformation, the equations are discretised and integrated using a control volume method.

For the advection terms, the values at the control volume faces are computed from the control volume centre using an advection scheme. There are two implemented schemes in the software: the hybrid scheme, which is a first-order scheme; and the QUICK scheme, third-order accurate. Despite producing more accurate results, the QUICK scheme is numerically less stable than the hybrid scheme.

After integrating, the equations are cast in the following general algebraic form:

$$a_P \phi_P = \sum_{nb} a_{nb} \phi_{nb} + b \tag{2.8}$$

This equation relates the generic variable ϕ, which can represent velocity components, turbulence quantities, or temperature, on a given location, P, with its neighbours' values, nb.

For numerical stability, the previous equations must be sub-relaxed. WindStation provides two sub-relaxation methods: the E-factor method, which has shown to provide better convergence speed for neutral atmosphere; and the false-transient method, which is better for non-neutral atmosphere.

The equations are then solved numerically using the SIMPLEC algorithm developed by Van Doormaal and Raithby in 1984, which is a variation of the original SIMPLE algorithm proposed by Patankar (1980). The method is applied using the Rhie-Chow (1983) interpolation procedure, with the modification proposed by Majumdar (1988).

The iterative process is considered as converged when all the normalised residual values are lower than a value R_{conv} predefined by the user, as present in eq. (2.9).

$$Max(R_u, R_v, R_w, R_m, R_k, R_\varepsilon, R_\theta) < R_{conv} \tag{2.9}$$

2.3. WindStation Features

In this subchapter, WindStation's features and tools that help its user to set up the problem are presented. These features are described in more detail in the User's Manual, Lopes (2020).

2.3.1. Digital Terrain Model

To define the digital terrain model, WindStation makes use of an elevation map. This map represents the height of the terrain relative to the height of sea level. There are also optional maps that can be used to define other terrain properties, such as roughness, forest model Cd×Lad, surface temperature, and surface heat flux.

In the present thesis, an elevation and a roughness map were used, since they are the most relevant for the studied problem. For its implementation, a WindStation feature that

allows importing both maps from online databases was used. SRTM elevation data and CORINE roughness data are imported from a governmental internet site and a menzio internal server, respectively. Both data are saved in ArcInfo ASCII Grid file format and loaded by WindStation.

2.3.2. Calculation Domain and Mesh

The calculation domain is the volume in which the numeric model calculates the wind flow. Mesh refers to the division of the domain where the numeric calculation occurs. Figure 5 and Figure 6 represent two similar domains with different horizontal and vertical mesh sizes. The presented figures demonstrate that the most refined mesh provides a better approximation of the terrain elevation, making its numeric simulation closer to the real problem.

WindStation uses a rectangular domain that can be automatically aligned with the direction of the wind. The horizontal mesh is in a Cartesian coordinate system and is evenly spaced. The vertical mesh has variable spacing, being more spaced with increasing height. Furthermore, WindStation can simplify the mesh configuration with features that automatically define the number of vertical levels, the height of z top, and the height of the first node.

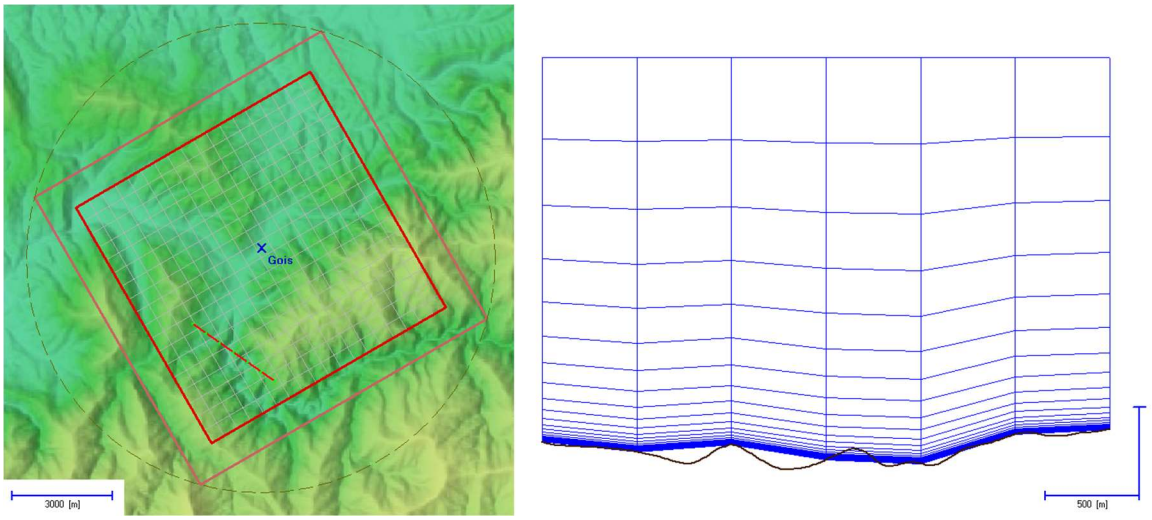

Figure 5 - Calculation domain with a low mesh resolution (450m horizontal mesh and 24 vertical levels).

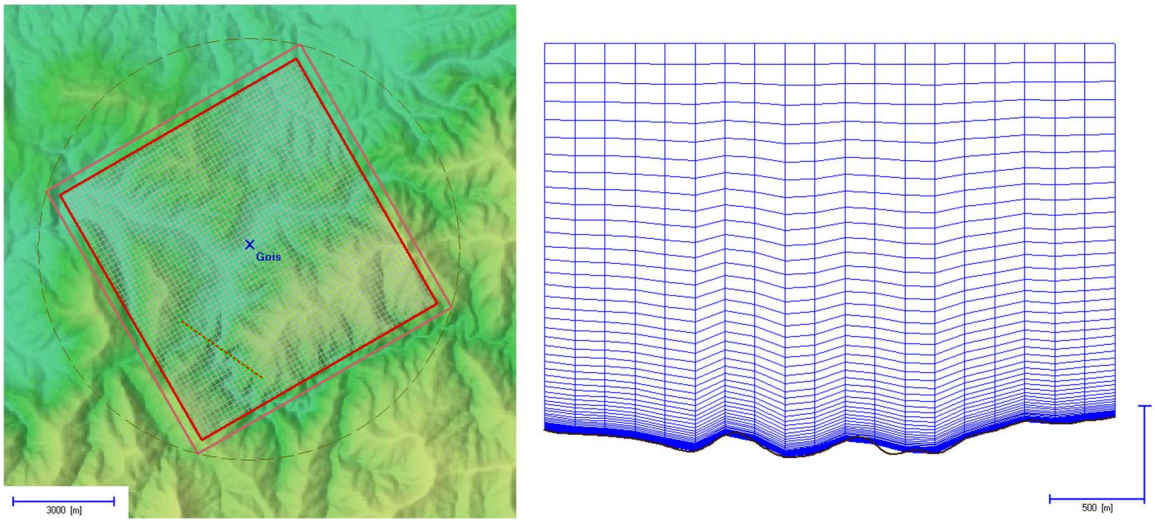

Figure 6 - Calculation domain with a high mesh resolution (150m horizontal mesh and 50 vertical levels).

2.3.3. Boundary Conditions and Problem Physics

For a simulation to represent more accurately the problem in study, the boundary conditions and the physics of the problem need to be well defined. In WindStation, the user can define the conditions of the top and lateral boundaries and enable or disable the Coriolis forces. Furthermore, WindStation includes definitions of initialisation parameters, such as input correction and nesting features, atmospheric stability, surface roughness and forest model, and ground temperature and flux.

In this section, an overview of the more relevant problem defining features is described.

Input Correction. As input data of the calculations, a meteorological station dataset is used. This dataset contains the station's location as coordinates, the wind speed, and the wind direction for a given time interval, and it is used as initialisation for the calculations. To approximate the simulation predictions to the input data, WindStation has an input correction feature. This feature rectifies the predictions by comparing the input data with the results at the same location, and, if needed, repeats the calculations with the corrected data. The user can define a maximum number of corrections and the threshold difference between the results and the input, required for the implementation of the input correction.

Nesting. WindStation allows the use of results from another simulation, usually with a larger domain and a less refined mesh named *LowRes* domain, as input data for the calculations. This process is designated by nesting. The purpose of the nesting feature is to simulate more complex sections of the terrain without the need to refine the mesh on the whole domain. This feature is usually implemented to help achieve more precise results in large calculation domains. Additionally, it can make the simulations less time consuming and more efficient if its application is thoughtfully planned.

Atmospheric Stability. For the atmospheric stability, WindStation gives the possibility to choose between three different options: neutral atmosphere, Monin-Obukhov (MO) length, and custom. The neutral atmosphere assumes that the potential temperature is constant with height, giving the possibility to change the sea-level temperature. In the Monin-Obukhov length, the potential temperature profile is provided by the MO theory. The custom option allows the user to define the temperature profile.

Forest Model. WindStation can use a forest model to simulate flows through porous materials, such as trees and bushes. When this model is used, some terms need to be acknowledged. The term Z_0 represents the roughness length, provided by the roughness map presented in Chapter 2.3.1. Z_f is the forest height and is calculated by the factor Z_f/Z_0, which takes the value of 20 by default but can be changed by the user. Z_0 threshold represents the minimum value of Z_0 necessary to activate the model. Cd×Lad, or forest type, expresses the permeability of the forest obstacle. In the used version of WindStation, the forest type is divided into four options: very sparse, slightly sparse, slightly dense, and very dense. A user-defined value can also be used.

Coriolis Effect. In WindStation, the Coriolis effect can be activated before the simulations as it can produce more realistic results. The latitude of the simulation location must be specified.

2.3.4. Climatology Calculation

Climatology is the scientific study of wind statistics over a period of time. In this thesis, a climatology approach was used, because it represents better the wind behaviour on meteorological stations and is more commonly used in the wind industry.

WindStation uses a computing feature entitled Climatology Calculation, which uses as input wind statistics of the meteorological station and simulates the wind statistics for the whole domain. The wind statistics data is divided by wind speeds (bins), and wind direction (sectors), and contains the occurring frequency of each combination of bins and sectors. In the Climatology Calculation, WindStation only calculates a selected number of bins of each sector. When all the simulations are concluded, WindStation computes a linear approximation of the remaining bins and calculates wind statistics for each point of the domain.

If Coriolis effects are not included, the solution is proportional to the input wind speed, thus computing only one bin produces valid results. Otherwise, if Coriolis effects are introduced, the use of at least 3 or 4 bins is recommended for more reliable results.

For climatology calculations, input correction should be used with the input station belonging to the calculation domain, as it improves the results. Additionally, the nesting feature can be used and does not require having the input station on the high-resolution domain.

3. RESOLUTION METHOD

In this chapter, the considered data, the methodology, and the software and hardware are described. In short, meteorological data was provided and evaluated, originating two possible case studies: the first case with three meteorological stations situated at 10 meters high in the central region of Portugal; and the second case that was implemented with the nesting feature and included the meteorological station of Penhas Douradas, situated on a mountain. The purpose of this second case study is to introduce more elevated wind measurements. WindStation simulated predictions for different input parameters in both cases, and the results were evaluated by comparison with the measured data using a climatology approach.

3.1. Climatology Data

The WindStation evaluation study was carried out using meteorological data provided by IPMA, CIM Coimbra, and CIM Viseu. In total, they contributed with information from 17 meteorological stations of Portugal's centre region for the years 2017 and 2018. The stations' measurements were collected at 10 meters high and provided with 10 minutes averaged time intervals. Although the height of the measurements is not ideal, due to lower wind speeds and higher variations in wind directions near the earth's surface, these represent real situations that are commonly used when studying the climate.

For the location of the study, a minimum of two meteorological stations with at least one full year of concurrent data each was defined as a prerequisite. Locations with greater station density were preferred to decrease the area of the simulation, reducing its time. The full year of concurrent data was used to allow the observation of the wind's behaviour through all the seasons, granting a better overview and analysis of the wind on the chosen location.

Regarding the mentioned prerequisites, the annual data of each meteorological station was inspected, and the stations with 85% or more of available yearly data were considered valid. The percentages of the available data are present in Table 1, with the

invalid years of each station marked in grey. Maps with the valid stations' location for the years of 2017 and 2018 are present in Figure 7 and Figure 8, respectively.

Table 1 - Meteorological stations and their data availability in percentage.

Meteorological Stations	2017	2018
Anadia / Estação Vitivinícola da Bairrada (IPMA)	100	75
Ansião (IPMA)	99.8	95.6
Arganil / Aeródromo (CIM Coimbra)	0	97.7
Arouca (IPMA)	94.7	95.5
Aveiro / Universidade (IPMA)	0	75.1
Carregal do Sal (CIM Viseu)	0	41.3
Coimbra / Aeródromo (IPMA)	99.2	98.6
Góis / Quinta da Ribeira (CIM Coimbra)	0	93.7
Lousã / Aeródromo (IPMA)	99.9	100
Mortágua / Aeródromo (CIM Coimbra)	0	84.6
Nelas (IPMA)	99.9	100
Oliveira do Hospital (CIM Coimbra)	0	19.8
Pampilhosa da Serra (IPMA)	57.6	47.8
Penacova / Hombres (CIM Coimbra)	0	99.3
Penhas Douradas / Observatório (IPMA)	97	87.6
Santa Comba Dão (CIM Viseu)	0	0.7
Viseu / Aeródromo (IPMA)	98.7	99.2

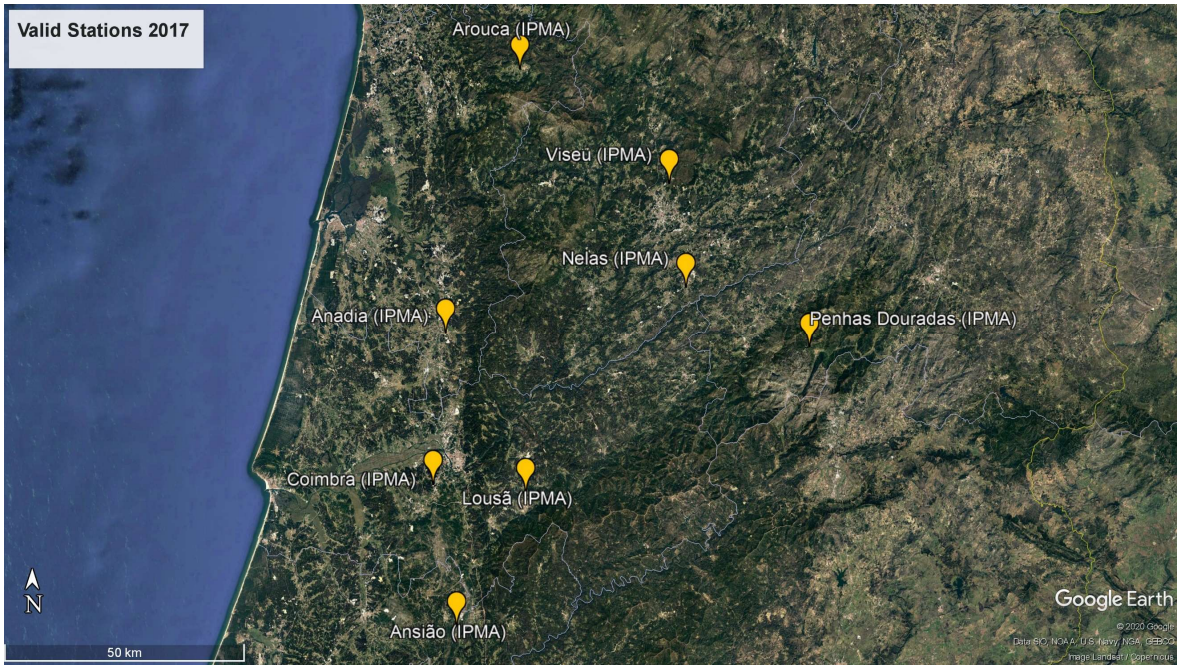

Figure 7 - Map with the valid meteorological stations for the year of 2017. Obtained from Google Earth.

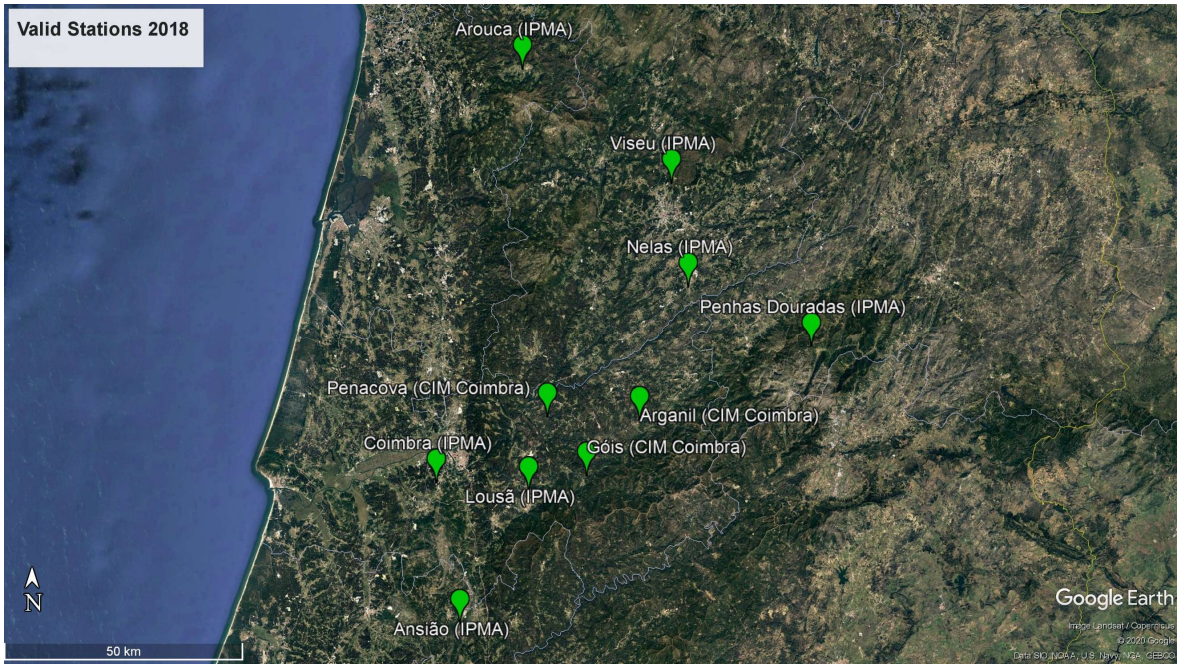

Figure 8 - Map with the valid meteorological stations for the year of 2018. Obtained from Google Earth.

The meteorological stations present in the highest stations' density area were chosen from the valid stations for one of the years. The chosen stations were Arganil / Aeródromo (CIM), Góis / Quinta da Ribeira (CIM), and Penacova / Hombres (CIM) for the year of 2018. The station of Penhas Douradas / Observatório (IPMA) in 2018, was also included in the second case study. For the remaining of the present thesis, the selected stations are referred by their location: Arganil, Góis, Penacova, and Penhas Douradas. Although the station of Lousã / Aeródromo (IPMA) belongs to the same location of the selected stations, it was not included in the evaluation studies, because during a preliminary analysis this station produced poor results, mainly due to low values of wind speed.

To verify the data integrity of the chosen meteorological stations, a quality control procedure, used in Giovannini et al. (2014) and reported in Jiménez et al. (2010), was applied. No invalid data was found, which led to the assumption that the data had a previous quality check. Hence, no alterations were made to the measured data.

For the climatology study, two methods were proposed: A 20-year and a 1-year assessment method. The 20-year method allows for an assessment for 20 years of meteorological data, which is more common and useful in the wind industry. For this method, the software windPRO, from EMD International A/S, was used. windPRO uses an MCP (Measure-Correlate-Predict) module, explained in Thøgersen et al. (2010) and Nielsen

et al. (2020), which correlates the short-term measurements with a precalculated long-term data, and predicts an approximation of both data for a 20-year time frame. Although the 20-year method would provide a broader range of wind results, therefore providing a better case study, the correlation between the short-term and long-term data was not ideal, resulting in a prediction that did not represent the measured data. The 1-year method assesses the data for 1 year and allows using only the original measurements. This method was used for this study.

To run the Climatology Calculation in WindStation, the input measurements needed to be converted into wind statistics. For this, windPRO was used to transform the measurement data from a time series format into a wind statistics file (.tab). The produced wind statistics were divided into 12 sectors with 30º intervals, and bins with 1 m/s intervals. Figure 9, Figure 10, Figure 11, and Figure 12 represent the wind rose with the occurrence frequency of each sector (a) and the Weibull frequency distribution of the wind speed (b). In the Weibull distribution (b) the bars represent the frequency, f [%], for each wind speed, u [$m.s^{-1}$], the values on the side A and k define the Weibull curve, the value U [$m.s^{-1}$] is the mean wind speed, and P [$W.m^{-2}$] is the estimated power. Furthermore, the tables with the complete statistic values are presented for each station in APPENDIX A.

Arganil / Aeródromo (CIM) [2018]

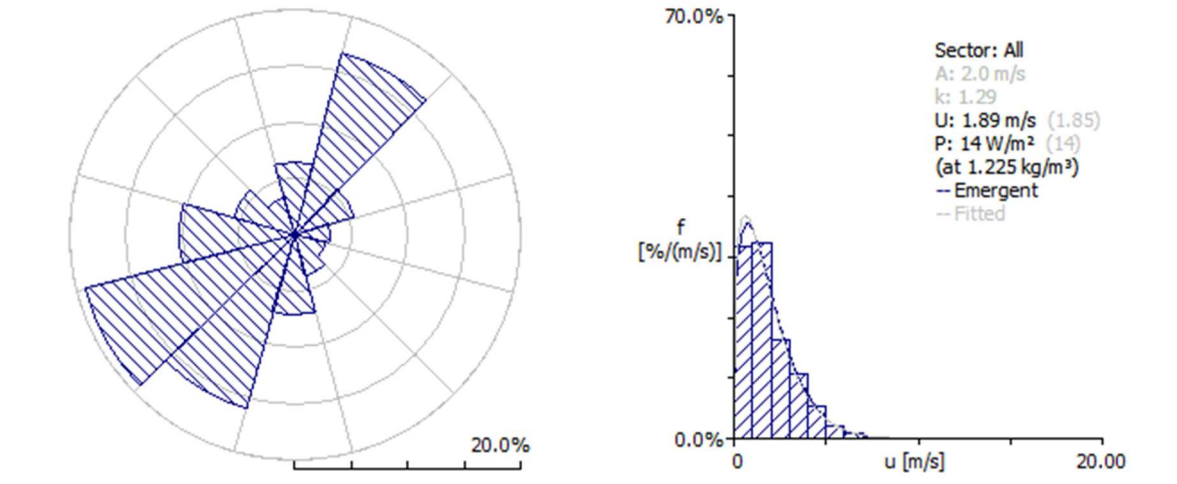

(a) (b)

Figure 9 - Wind rose frequency distribution (a) and Weibull distribution of the wind speed (b), for the meteorological station of Arganil. Obtained from WAsP 12.5.

Góis / Quinta da Ribeira (CIM) [2018]

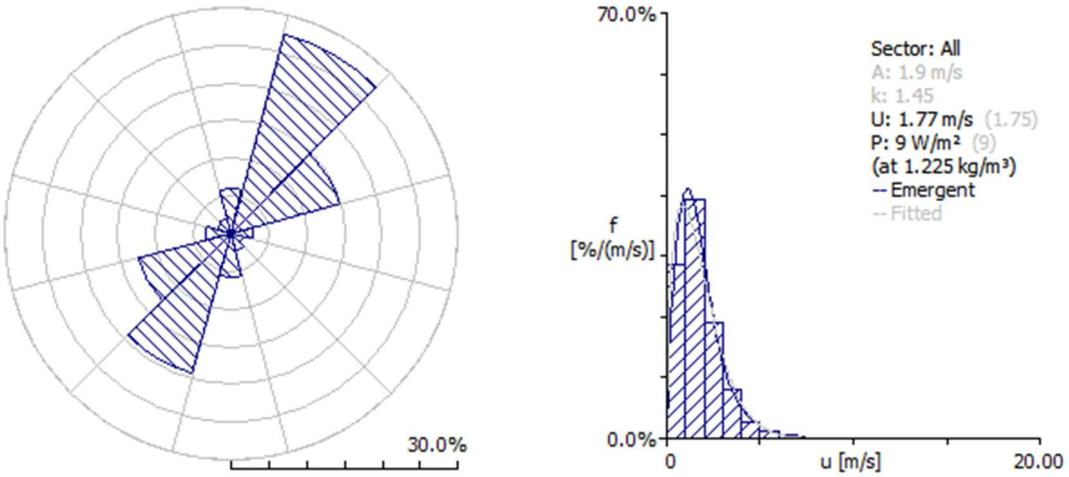

(a) (b)

Figure 10 - Wind rose frequency distribution (a) and Weibull distribution of the wind speed (b), for the meteorological station of Góis. Obtained from WAsP 12.5.

Penacova / Hombres (CIM) [2018]

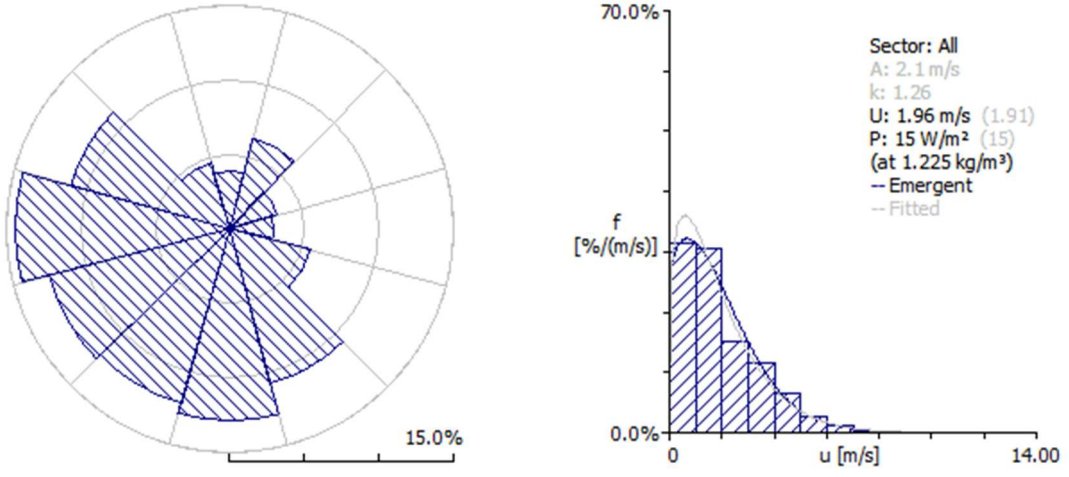

(a) (b)

Figure 11 - Wind rose frequency distribution (a) and Weibull distribution of the wind speed (b), for the meteorological station of Penacova. Obtained from WAsP 12.5.

Penhas Douradas / Observatório (IPMA) [2018]

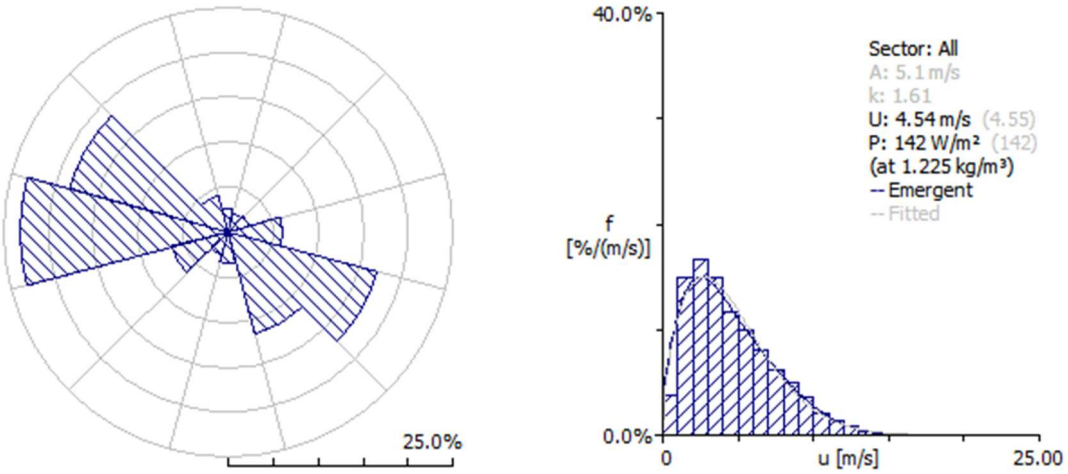

(a) (b)

Figure 12 - Wind rose frequency distribution (a) and Weibull distribution of the wind speed (b), for the meteorological station of Penhas Douradas. Obtained from WAsP 12.5.

3.2. Test Site

The test site, in central Portugal, has a complex hilly system with rivers flowing from east to west. It is mostly constituted by small hills and valleys, with peaks altitude of 500 meters. On the southeast half, it has a set of mountains that are around 1000 meters tall that end east with a maximum height of 2000 meters. The test site has variable roughness due to the presence of different terrain types. These can be natural forests, planted forests, cities and villages, plantations, rivers, and others.

As mentioned in the previous chapter, the tests locations contain three meteorological stations for the first case study and a fourth meteorological station, Penhas Douradas, for the second case study. The chosen test sites have meteorological data available from Arganil, and Góis, Penacova, and Penhas Douradas. Arganil and Penacova stations are located on top of small hills, the station of Góis is situated on a valley, and Penhas Douradas station is located in the highest mountain. The exact locations of the meteorological stations were verified with the help of satellite information, more specifically Google Earth. Their geographic coordinates are presented in Table 2.

Although the location with the higher meteorological station's density was chosen, in the first case's test site, the furthest stations are located at 20 kilometres from each

other. In the second case's test site, the station of Penhas Douradas is the furthest away at 38.5 kilometres from its closest station. Due to current hardware limitations, these distances can provide a challenge in the simulations when refining the mesh.

Table 2 - Location of the selected meteorological stations.

Metereological Stations	Latitude [°]	Longitude [°]	Elevation [m]
Arganil	40.2743310	-7.9741865	229.3
Góis	40.1715543	-8.1030321	190.6
Penacova	40.2809925	-8.1986950	143.0
Penhas Douradas	40.4115661	-7.5584683	1380.3

In WindStation, the elevation and roughness were imported with the inbuilt functionality mentioned in Chapter 2.3.1. A larger area was imported to provide flexibility when defining the calculation domain. The first and second case's *HighRes* domains are identical and were defined horizontally as a 36.6 kilometres wide square and vertically with 4400 meters in height. For the second case, a *LowRes* domain is included due to the use of the nesting feature. It was defined with 79.2 kilometres wide and 9600 meters high. Figure 13 represents the *HighRes* (a) and *LowRes* (b) domains, containing the elevation map, the locations of the referred meteorological stations, and the domain borders. Figure 14, Figure 15, Figure 16, and Figure 17 represent the elevation (a) and roughness (b) maps, surrounding each meteorological station location.

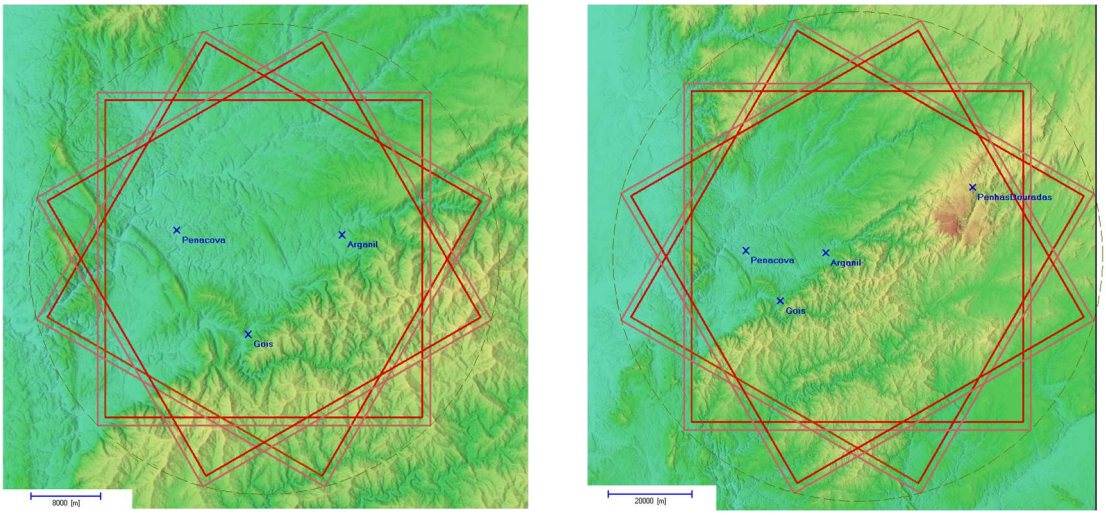

(a) (b)

Figure 13 - *HighRes* (a) and *LowRes* (b) domains with the elevation map, the domain borders, and the meteorological stations' location.

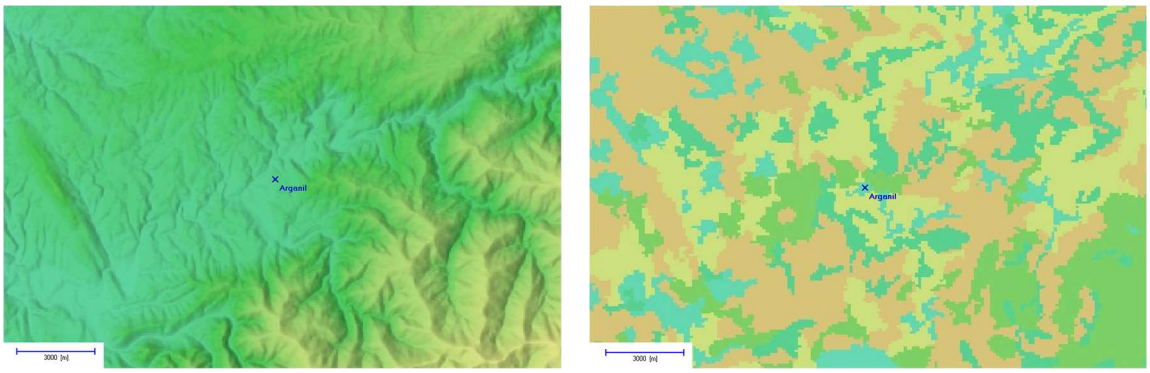

(a) (b)

Figure 14 -Elevation (a) and roughness (b) maps surrounding the meteorological station of Arganil.

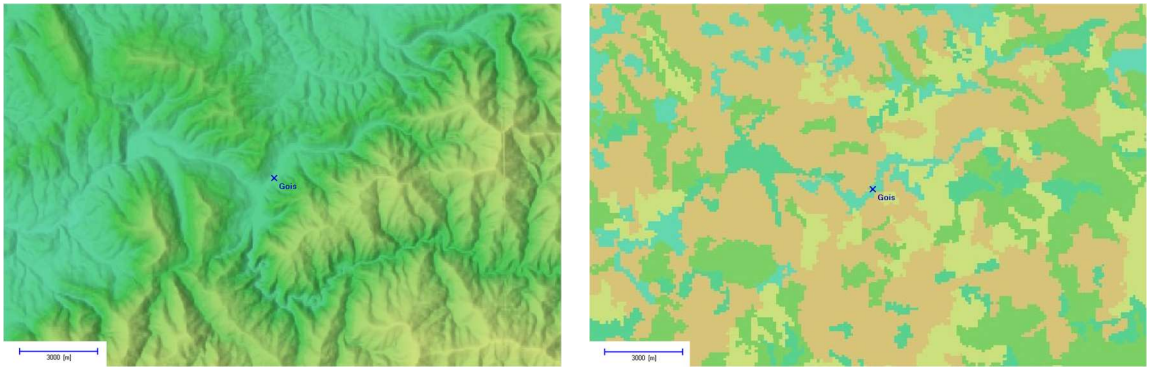

(a) (b)

Figure 15 - Elevation (a) and roughness (b) maps surrounding the meteorological station of Góis.

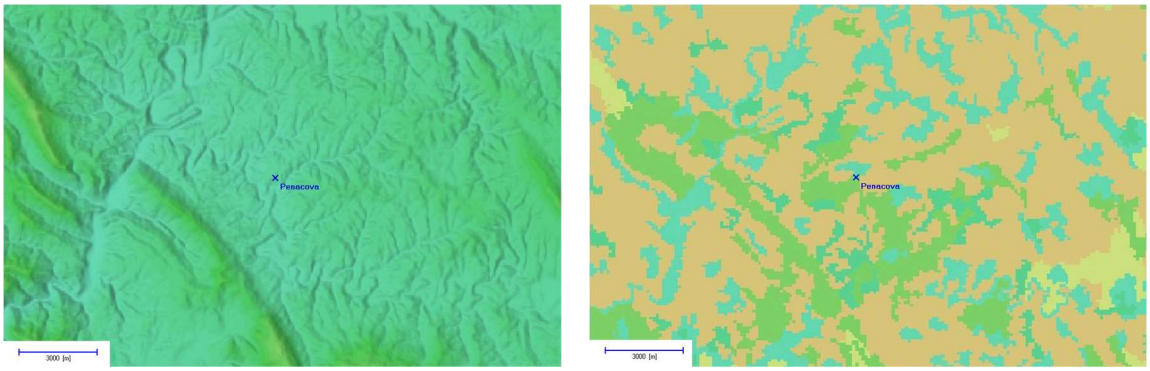

(a) (b)

Figure 16 - Elevation (a) and roughness (b) maps surrounding the meteorological station of Penacova.

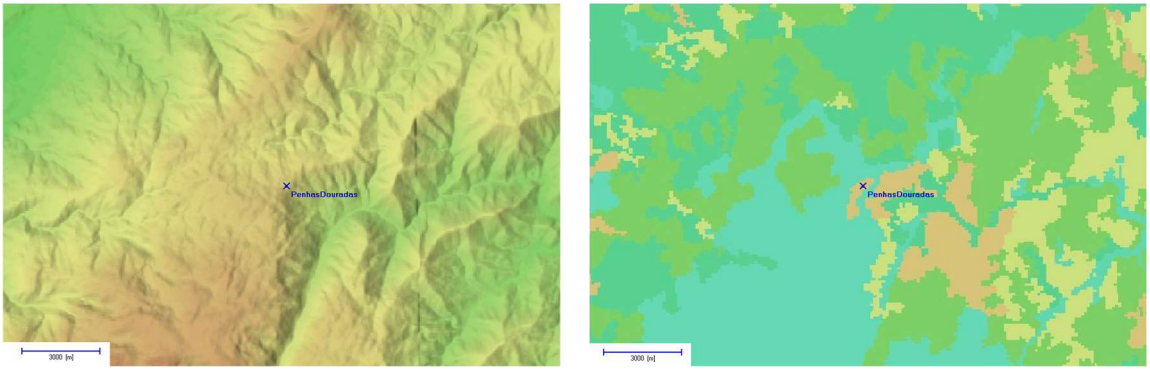

(a) (b)

Figure 17 - Elevation (a) and roughness (b) maps surrounding the meteorological station of Penhas Douradas.

3.3. Sensitivity Analysis

The goal of the sensitivity analysis is to study the influence of specific parameters on the simulation time and results. This analysis allows verifying which parameters are more relevant to obtain better results. In sum, a prior mesh analysis was introduced in the *HighRes* domain to optimise the *LowRes* and *HighRes* meshes, as they both have a similar terrain composition. The following analyses were executed comparing the result when using different meteorological station data as input. The first case, in the *HighRes* domain, studied the wind climatology for Arganil, Góis, and Penacova stations, and, the second case, using the nesting feature and a *LowRes* domain adding the station of Penhas Douradas.

Some parameters were used throughout all the sensitivity analyses unless stated otherwise in the test's description. As a default, for the calculation domain, the previously mentioned sizes were used. The *HighRes* domain was defined with 36.6 by 36.6 by 4.4 kilometres and a first lower node at 1.8 meters high. The *LowRes* domain was defined with a size of 79.2 by 79.2 by 9.6 kilometres and a first lower node at 2.8 meters high. In both tests, the domain was automatically aligned to face the wind direction.

For the problem physics, the simulations did not include Coriolis effects nor Forest model. Thus, only 1 bin per sector was used to compute the simulation. Additionally, neutral atmosphere was considered due to the variety of temperature profiles throughout the year.

For the numerical model, a residual convergence test, mentioned in the mesh analysis, proved that a maximum convergence residual of 1E-4 for the less refined meshes and 5E-5 for the more refined meshes was ideal. Also, a maximum of 1500 iterations was established. Furthermore, the standard k-ε turbulence model, the hybrid advection scheme, and, as sub-relaxation, the automatic E-Factor method were used.

3.3.1. Mesh Analysis

Usually, a more refined mesh provides more terrain information, conceding more realistic results. Unfortunately, this refinement leads to more nodes, increasing the number of calculations and processing time. This problem motivates the first sensitivity test, which studies the influence of the mesh refinement of both horizontal and vertical grids. The objective is to verify this phenomenon and the possibility to use a less refined mesh without compromising the results and saving processing time.

For this analysis, the refinement influence of the horizontal and vertical mesh was verified separately, varying the horizontal mesh size and vertical levels, respectively. Additionally, the maximum convergence residual value was tested and verified for each mesh size to confirm the convergence of the results. The default parameters of the *HighRes* domain were used, and the station of Penacova was defined as the input station due to its higher percentage of available data. After the analysis, the most suitable mesh resolutions were chosen for the following sensitivity tests.

3.3.2. Low-Altitude and High-Altitude Input Stations Analysis

Multiple meteorological stations can be used simultaneously as an input. In that situation, the input correction feature uses the data of the selected stations belonging to the calculation domain and provides an average correction of the stations.

After the optimisation of the mesh sizes, the WindStation's behaviour was studied for the utilisation of different input stations. This analysis allows verifying if the use of multiple input stations provides more realistic results when compared to the use of a single input station, which requires less processing time. Furthermore, two case-studies with stations at different heights were presented to study the influence of high-altitude measurements on the results.

With this purpose, the first case used the low-altitude stations of Arganil, Góis, and Penacova. The simulations were performed with the optimised mesh size selected from the previous mesh analysis and using the default parameters and the *HighRes* domain. All the different combinations of input stations were simulated, leaving at least one station as output to evaluate the results.

In the second case, due to the lack of wind measurements at high altitude and, consequently, lack of high wind speed velocities, the meteorological station of Penhas Douradas was introduced. In order to optimise the processing time and allow the assessment of the result in a comparable mesh resolution, the nesting feature was implemented with the mentioned *LowRes* and *HighRes* domains. The nesting feature simulated both domains separately. The *LowRes* domain utilised the meteorological Penhas Douradas station as input and used its default parameters. Additionally, similarly to the previous analysis, combinations of multiple input stations were tested, always including Penhas Douradas. The second simulation of the nesting feature, with the *HighRes* default parameters, included the results of the respective *LowRes* simulation and the input stations belonging to its domain. In this second simulation, Penhas Douradas station was only used for initialisation, as it does not belong to the *HighRes* domain.

3.4. Results Comparison and Evaluation

After climatology simulations, WindStation provides the results as statistical data on the whole domain. The values of mean wind speed, *WSpd*, and wind direction frequency, *DFreq*, for each sector, were considered necessary to these studies, as they provide useful information on the wind's behaviour. The *WSpd* values could also be compared as a total average in all directions, but those values were not deemed relevant, as they provide lesser information when examining the wind speed.

In the mesh analysis, the results were compared between simulations with different mesh sizes. A convergence of the results is expected with the increase in the number of calculation nodes. For this analysis, since the results are provided in statistical data, the *WSpd* and *DFreq* values were compared in each sector for Arganil and Góis stations. Furthermore, the processing time associated with the number of nodes in a simulation was considered when selecting an optimised mesh size.

The remaining sensitivity analyses were based on Wallbank (2008), where the simulation results, both *WSpd* and *DFreq*, were compared with their respective measurements in each sector. Due to a larger variation of the mean wind speeds used throughout different commercial scenarios, the *WSpd* comparisons were presented in a percentage error format (cf. eq. (3.1)). For the *DFreq*, a more direct approach was used, since its values can range from 0% to 100%, creating a significant difference in error percentage for the lower values. For that reason, the *DFreq* error was defined by the difference between the measurements and predicted result, as present in eq. (3.2).

$$E_{WSpd} = \frac{WSpd_{predicted} - WSpd_{\text{measured}}}{WSpd_{\text{measured}}} \times 100 \tag{3.1}$$

$$E_{DFreq} = DFreq_{predicted} - DFreq_{\text{measured}} \tag{3.2}$$

Although the mentioned evaluation format is better when representing the analysis of specific sectors, a more global approach, with all the sectors, was required to compare the performance of the sensitivity tests. With this, to evaluate WindStation's performance in each station, the *WSpd* mean absolute percentage error and the *DFreq* mean absolute error of all sectors were used.

3.5. Software

In this study, a license for WindStation v1.4.13, provided by menzio GmbH, and an academic license for windPRO 3.3 by EMD International A/S, acquired by the University of Coimbra, were used. These licenses were used solely for this study. Furthermore, an academic license of Microsoft Office 365 ProPlus and an unlicensed version of WAsP 12.5 were used during the analysis of the measurements and results.

3.6. Hardware

To run the simulation models on WindStation, the author used two computers: Computer A, with an AMD Ryzen™ 7 3700X 8-Core 3.6GHz-4.4GHz processor, 16GB DDR4 RAM, and Microsoft Windows 10 Professional (x64) Build 19041.388 operating system; and Computer B, with an Intel® Core™ i7-5930K 6-Core 3.50GHz processor,

16GB DDR4 RAM, and Microsoft Windows 10 Professional (x64) Build 17763.805 operating system.

4. RESULTS AND ANALYSIS

The current chapter presents the results of the sensitivity study. The explanation of the performed analysis and the evaluation methodology is present in Chapter 3.3 and Chapter 3.4. In order to simplify the analysis and presentation of the results, not all the obtained results are shown in this chapter. The complete graphics analyses and results tables are presented in APPENDIX B and APPENDIX C, for the mesh analysis and remaining analyses, respectively.

4.1. Mesh Results

The study of the horizontal and vertical meshes was performed by varying the mesh size and the number of vertical levels, respectively. The mesh size, the vertical levels, and the remaining variable parameters are presented in Table 3 and Table 4, in conjunction with the simulation's processing time on the used computers, A and B. In the current section, only the sectors of 30º, 150º, and 270º are presented, as they are sufficient to obtain valid conclusions of the mesh study. The complete graphic analysis of the mesh tests is accessible in APPENDIX B.

Table 3 - Simulations parameters and processing times for the horizontal mesh analysis.

Simulation Name	Mesh Size [m]	Vertical Levels	Mesh Division	Nodes	Residual Convergence	Processing Time
Pena_M750.64_1e-4	750	64	49x49x64	153 664	1E-04	[A] 0h25
Pena_M600.64_1e-4	600	64	61x61x64	238 144	1E-04	[A] 0h16
Pena_M450.64_1e-4	450	64	81x81x64	419 904	1E-04	[B] 0h49
Pena_M300.64_5e-5	300	64	123x123x64	968 256	5E-05	[A] *
Pena_M210.64_5e-5	210	64	175x175x64	1 960 000	5E-05	[A] 4h21 / [B] 8h15
Pena_M150.64_5e-5	150	64	245x245x64	3 841 600	5E-05	[B] 17h42
Pena_M120.64_5e-5	120	64	305x305x64	5 953 600	5E-05	[A] 28h02 / [B] 34h23
Pena_M90.64_5e-5	90	64	407x407x64	10 601 536	5E-05	[A] +50h* / [B] +60h*

* Processing time not present or not accurate due to software errors or interruptions on the simulations.

Table 4 - Simulations parameters and processing times for the vertical mesh analysis.

Simulation Name	Mesh Size [m]	Vertical Levels	Mesh Division	Nodes	Residual Convergence	Processing Time
Pena_M150.20_5e-5	150	20	245x245x20	1 200 500	5E-05	[A] 1h30
Pena_M150.30_5e-5	150	30	245x245x30	1 800 750	5E-05	[A] 2h54
Pena_M150.40_5e-5	150	40	245x245x40	2 401 000	5E-05	[A] 3h59
Pena_M150.50_5e-5	150	50	245x245x50	3 001 250	5E-05	[B] 12h19
Pena_M150.64_5e-5	150	64	245x245x64	3 841 600	5E-05	[B] 17h42
Pena_M150.80_5e-5	150	80	245x245x80	4 802 000	5E-05	[B] +25h*

* Processing time not present or not accurate due to software errors or interruptions on the simulations.

Horizontal Mesh. Figure 18 and Figure 19 represent charts of the mean wind speed results in function of the number of nodes, of the horizontal mesh study for the stations of Arganil and Góis, respectively. Through the examinations of the referred charts, the following observations were made:

- The variation of the mesh size affected each sector differently, which means that more than one sector needs to be considered to verify possible conclusions.
- In the station of Góis, some values offered a challenge to simulate, as shown in Góis sector 150 and 270 for the more refined meshes, with 300 meters or less mesh size. The null values probably occur due to the station's location in a valley, creating a difficulty to process winds originated from the side hills.
- The wind speed results varied up to 0.4 m/s between mesh sizes in Arganil sector 270 and Góis sector 30, which is substantial for wind speeds of 2 and 3 m/s. With these discrepancies, the horizontal mesh size can be considered a highly influential parameter.
- Smaller discrepancies between results were expected with the increase in the number of nodes. Unfortunately, in Arganil Sector 270, the mean wind speed variation did not seem to be decreasing with the number of nodes, leading to the assumption that a more refined mesh was necessary.

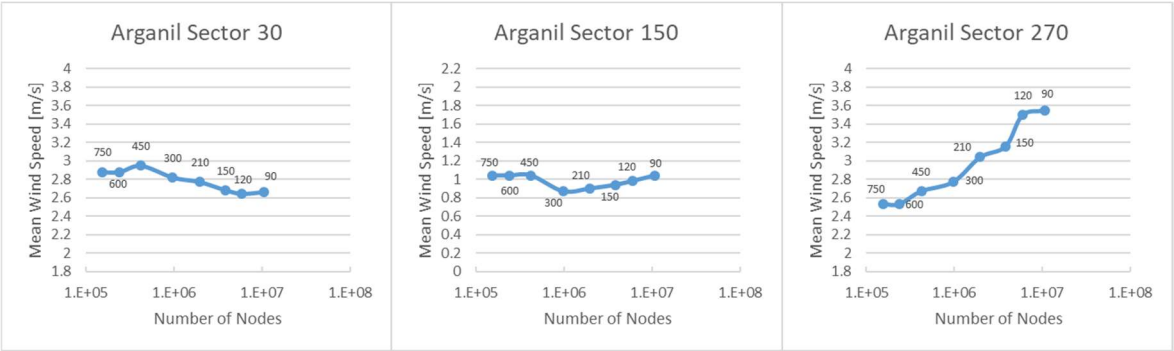

Figure 18 - Horizontal mesh analysis in Arganil sectors 30, 150, and 270.

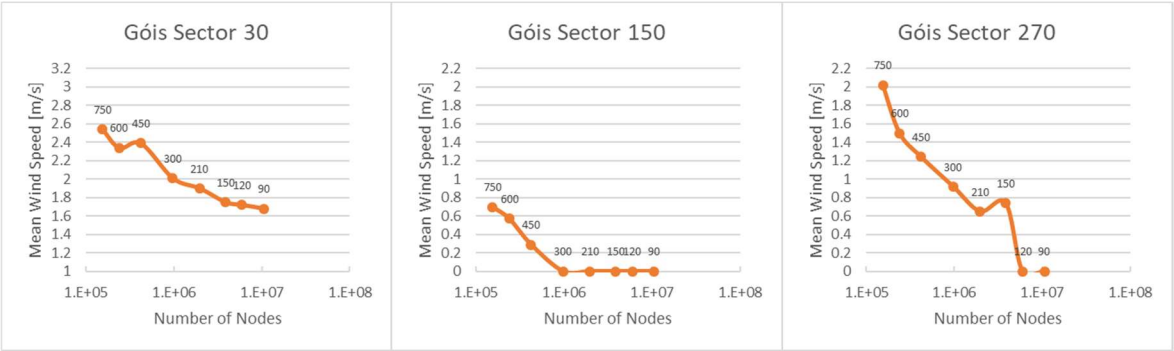

Figure 19 - Horizontal mesh analysis in Góis sectors 30, 150, and 270.

Vertical Mesh. Similarly to the horizontal mesh size, Figure 20 and Figure 21 represent the results charts of the vertical mesh tests for the stations of Arganil and Góis. Through the analysis of these charts, the following observations were made:

- Once more, the simulation proved to have difficulty calculating the wind velocity for some sectors in the station of Góis, as shown in Góis sector 150.
- In comparison with the horizontal mesh test, the results varied less, with a maximum variation of 0.1 m/s wind speed, concluding that the vertical mesh refinement is substantially less influential than the horizontal mesh refinement.
- Contrary to the horizontal mesh observations, the mean wind speed results tended to converge with the increase of the number of nodes. Although the results in Arganil sector 150 and 270 are not exactly constant, their variation is relatively small. This observation proves that the results of simulations with 30 vertical level mesh or more can be used, improving the processing time without harming the precision of the results.

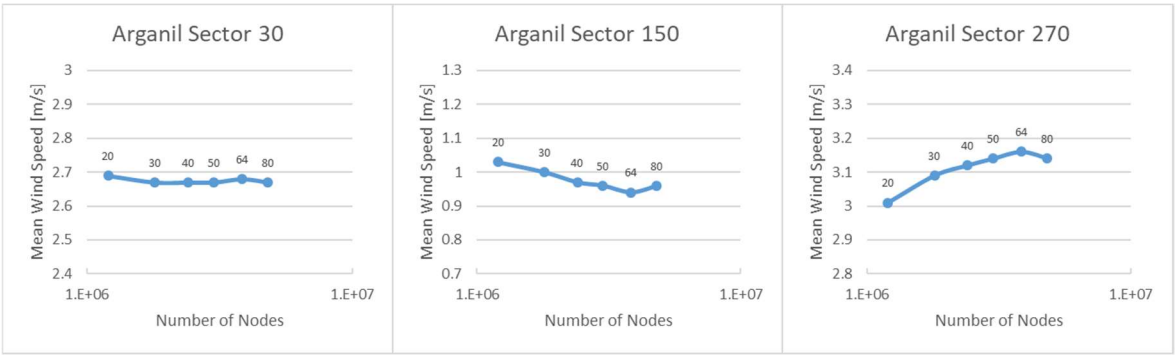

Figure 20 - Vertical mesh analysis in Arganil sectors 30, 150, and 270.

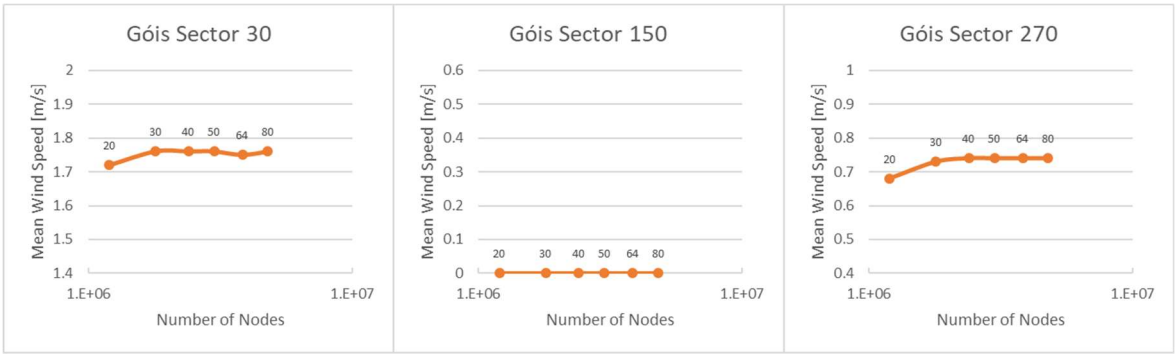

Figure 21 - Vertical mesh analysis in Góis sectors 30, 150, and 270.

To conclude the mesh analysis, the horizontal mesh refinement was not considered enough to verify the stability of the results and was a highly influential parameter. On the other hand, the vertical mesh converged and was considerably less influent on the variation of the results. Additionally, the observation of the processing time demonstrated a significant increase with the increase in the number of nodes.

In order to optimise the succeeding simulations, a selected mesh based on the processing time and previous observations was chosen. A larger vertical mesh was used to decrease the simulation time without negatively affecting the results. A more refined horizontal mesh was targeted to decrease its influence in the accuracy of the results. Table 5 represents the optimised mesh definitions for the *HighRes* and *LowRes* domains, that were used in the subsequent input stations sensitivity studies.

Table 5 - Optimized *HighRes* and *LowRes* domain and mesh parameters.

Test Site	Domain Size [km]	Mesh Size [m]	Vertical Levels	Mesh Division	Nodes	Residual Convergence
HighRes Domain	36.6 x 36.6 x 4.4	150	30	245x245x30	1 800 750	5E-05
LowRes Domain	79.2 x 79.2 x 9.6	300	40	265x265x40	2 809 000	5E-05

Residual Convergence. In addition to the mesh analysis, several residual convergence values were tested. Although the analysis is not presented for each mesh size and residual convergence value, the results were observed throughout the simulations to verify their convergence.

As an example of the convergence study, Figure 22 represents the wind speed and direction results throughout the simulations with Penacova as the input station, 210m horizontal mesh size, 64 vertical levels, and two residual values, 1E-4 and 5E-5 (Pena_M210.64_1E-4 and Pena_M210.64_5E-5). Additionally, Table 6 presents the percentage difference between the end results of both residual values simulations, for the wind speed and direction in all stations location, in sector 30 and bin 10. From the convergence analysis and presented figures, the following conclusions were taken:

- All the results remained relatively constant in the sections before a considerable value alteration, caused by the input correction, and in the end section of the simulation. This observation indicates that both 1E-4 and 5E-5 maximum residual values allow for the convergence of the simulation results.
- When comparing the number of iterations between 1E-4 and 5E-5 residual convergence, there was an increase of almost 39%, from 310 to 430 iterations. This increase is projected directly on the processing time.
- The percentual difference of the results is almost negligible, meaning that the use of a residual convergence of 5E-5 might not be ideal when compared to a lower residual convergence of 1E-4.
- Even though the result from different meshes is not presented, a necessity of lower residual convergence values for the convergence of more refined meshes was observed.

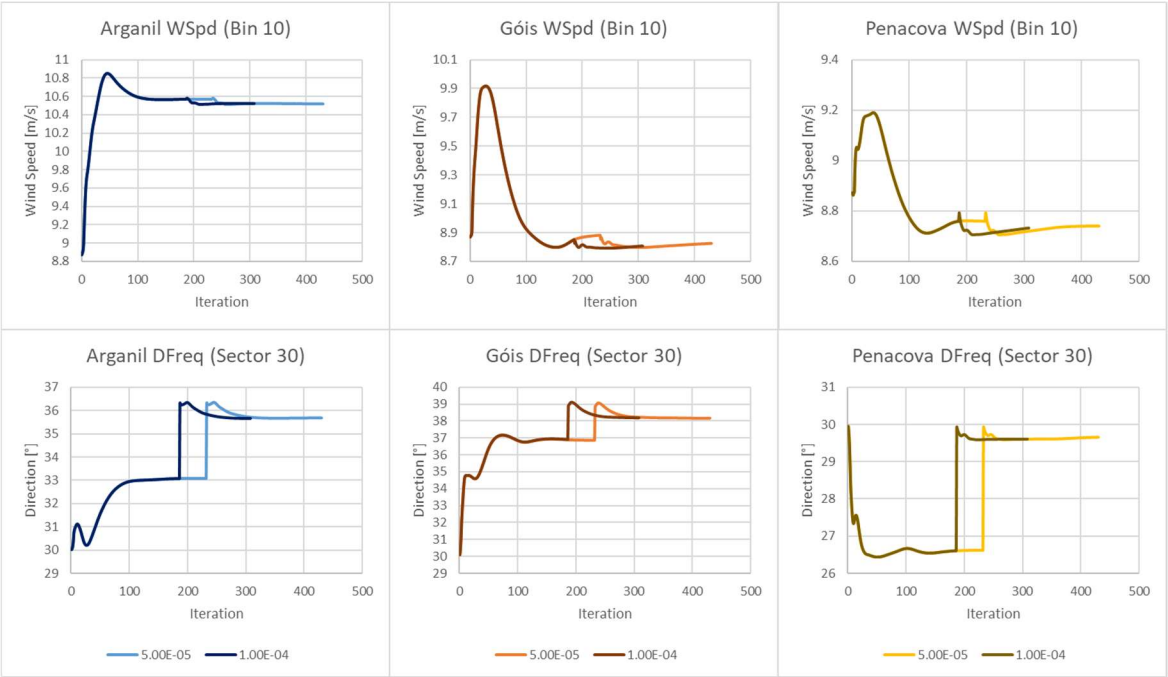

Figure 22 - Wind speed and direction results during the simulations of Pena_M210.64_1E-4 and Pena_M210.64_5E-5, for sector 30 and bin 10.

Table 6 - Percentage difference of the wind speed and direction ending results between Pena_M210.64_1E-4 and Pena_M210.64_5E-5, for sector 30 and bin 10.

End Result Differences in Percentage [%]

Station	Arganil	Góis	Penacova
Wind Speed Difference	0.04%	0.21%	0.08%
Direction Difference	0.04%	0.00%	0.17%

In order to choose the residual convergence value for the subsequent analysis, the previous observations were considered. For less refined meshes, the higher residual convergence value of 1E-4 was used, as shown in Table 3. Although this value also was proven to converge on more refined meshes, a more cautious approach was taken, as the preceding example could not be valid for all the different wind speeds, directions, and study locations. Thus, the residual convergence value of 5E-5 was used for the more refined meshes with less than 450m horizontal mesh size.

4.2. Results from Low-Altitude Stations

In this analysis, the results obtained from simulations with different input stations were compared with the data from the provided measurements. The simulations performed, their variable parameters, and processing times, for computer A and B, are presented in Table 7. The input station represents the data that was inserted in WindStation for processing, and the output station is the location where the comparative analysis occurs.

Table 7 - Simulations parameters and processing times for the low-altitude input stations analysis.

Simulation Name	Input Station(s)	Output Station(s)	Processing Time [min]
Arga_M150.30_5e-5	Arganil	Góis, Penacova	[A] 3h05 / [B] 5h09
Gois_M150.30_5e-5	Góis	Arganil, Penacova	[B] 5h04
Pena_M150.30_5e-5	Penacova	Arganil, Góis	[A] 2h39
ArgaGois_M150.30_5e-5	Arganil, Góis	Penacova	[A] 8h14
ArgaPena_M150.30_5e-5	Arganil, Penacova	Góis	[A] 6h42
GoisPena_M150.30_5e-5	Góis, Penacova	Arganil	[A] 9h03

Table 8 presents the comparison results in each station's location given in an error format, as described in Chapter 3.4. Figure 23, Figure 24, and Figure 25 represent sector-based comparison charts on the stations of Arganil, Góis, and Penacova, respectively. The top charts represent the result values of *DFreq* (a) and *WSpd* (b), and the station's measurements. The bottom charts represent the calculated error of both *DFreq* (c) and *WSpd* (d). All the results and error values are present in APPENDIX C. From the observation of the mentioned figures, the following conclusions were made:

- The mean errors of *DFreq* and *WSpd* were not directly related, as can be seen when examining the results in Arganil station and, even more noticeable, in Góis station. A present example is the simulation Pena_M150.30_5E-5, that, when analysing the stations' location of Arganil and Góis, it achieves the best results of *WSpd* for both stations, but performs weakly in *DFreq*, giving the worst results for *DFreq* in Góis.
- Due to its location, the problem mentioned when predicting the results for the station of Góis is noticeable. The results of *WSpd* for some sectors is 0 m/s, as the terrain and the low speeds and probability of the valley side winds offer a

challenge to the software. Furthermore, due to the stated problem, Góis, when used as a solo input station, provides the worst results from all input stations.

- In this study, the results closest to the measurements were provided by Arga_M150.30_5E-5 when examining Penacova's location, with errors of 3.73 for *DFreq* and 27.7% for *WSpd*. Pena_M150.30_5E-5 provided similar errors for Arganil station, but the use of multiple stations, GoisPena_M150.30_5E-5, decreased the *DFreq* error from 3.88 to 2.59 and increased the *WSpd* error from 30.7% to 40.5%.
- Although the use of multiple stations improved some results, as seen in the *DFreq* in Arganil and Góis location, from the simulations GoisPena_M150.30_5E-5 and ArgaPena_M150.30_5E-5 respectively, no overall improvements were verified. The use of multiple input stations, in most cases, provided an averaged prediction between the input stations used, as can be seen in the most graphs of the *WSpd* and *DFreq* results.
- An increase of the processing time can be observed in simulations with multiple stations input. This increase occurs due to the necessity to compute the results from two input stations, doubling the processing time.

Table 8 - *DFreq* and *WSpd* mean errors from the simulations with low-altitude input stations.

Simulation Name	Arganil Station		Góis Station		Penacova Station	
	DFreq Mean Error	WSpd Mean Error [%]	DFreq Mean Error	WSpd Mean Error [%]	DFreq Mean Error	WSpd Mean Error [%]
Arga_M150.30_5e-5	-	-	4.66	78.8	3.73	27.7
Gois_M150.30_5e-5	3.99	68.9	-	-	5.46	84.9
Pena_M150.30_5e-5	3.88	30.7	5.12	57.6	-	-
ArgaGois_M150.30_5e-5	-	-	-	-	4.27	53.0
ArgaPena_M150.30_5e-5	-	-	4.30	61.1	-	-
GoisPena_M150.30_5e-5	2.59	40.5	-	-	-	-

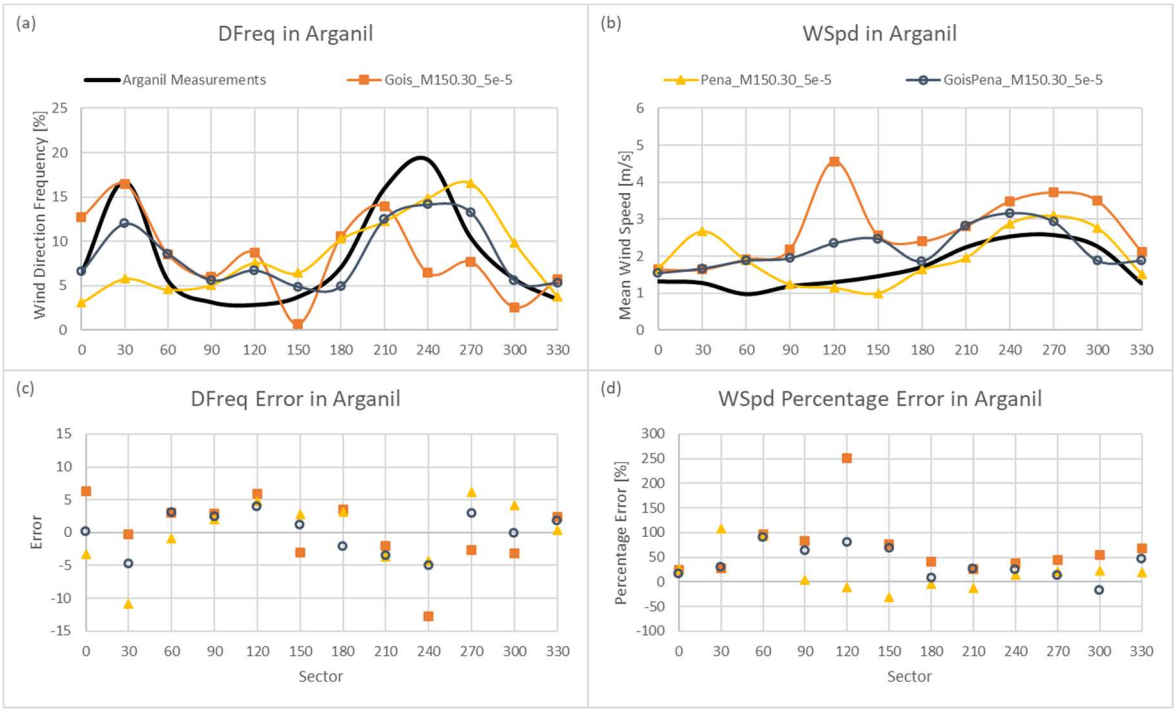

Figure 23 - *DFreq* (a) and *WSpd* (b) results and *DFreq* (c) and *WSpd* (d) errors of the low-altitude input stations analysis, in Arganil.

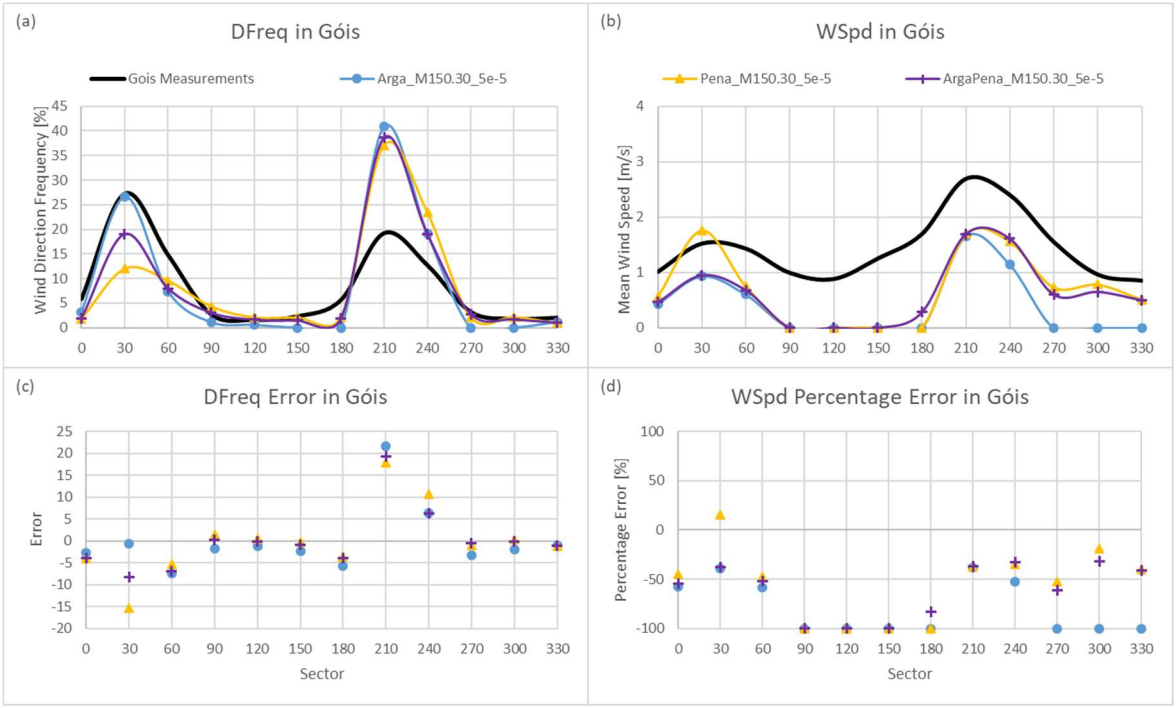

Figure 24 - *DFreq* (a) and *WSpd* (b) results and *DFreq* (c) and *WSpd* (d) errors of the low-altitude input stations analysis, in Góis.

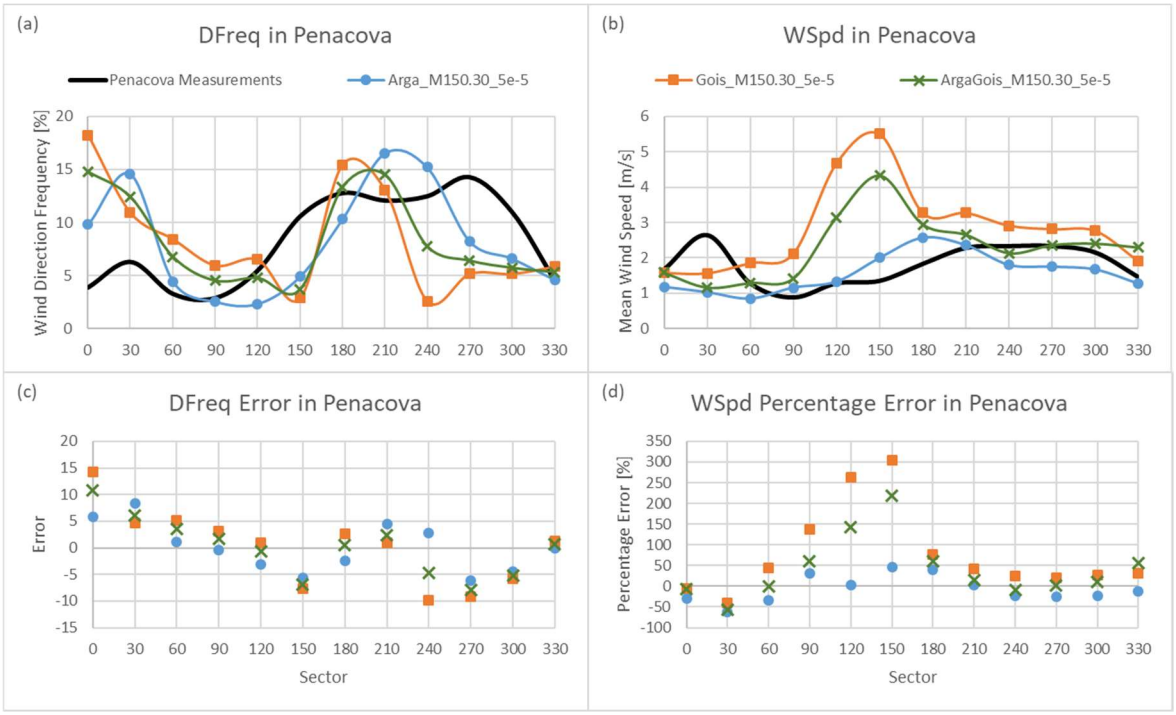

Figure 25 - *DFreq* (a) and *WSpd* (b) results and *DFreq* (c) and *WSpd* (d) errors of the low-altitude input stations analysis, in Penacova.

4.3. Results from the Inclusion of a High-Altitude Station

The analysis with the inclusion of Penhas Douradas station was performed using the nesting feature. The nesting simulation was performed separately in the *LowRes* and *HighRes* domains. Similar to the previous input stations analysis, this study consisted of using different input stations. Table 9 represents the performed simulations with the input and output stations and the processing time required for each *LowRes* and *HighRes* simulations, in computer A and B.

Table 9 - Simulations parameters and processing times for the inclusion of a high-altitude input station analysis.

Simulation Name	Input Station(s)	Output Station(s)	Processing Time		
			LowRes	HighRes	Total
Nst_PDou_M150.30_5e-5	Penhas Douradas	Arganil, Góis, Penacova	[B] 14h29	[B] 2h10	[B] 16h39
Nst_PDouArga_M150.30_5e-5	Penhas Douradas, Arganil	Góis, Penacova	[B] 23h14	[B] 5h31	[B] 28h45
Nst_PDouGois_M150.30_5e-5	Penhas Douradas, Góis	Arganil, Penacova	[A] 16h42	[A] 5h38	[A] 22h20
Nst_PDouPena_M150.30_5e-5	Penhas Douradas, Penacova	Arganil, Góis	[A] 14h24	[A] 5h42	[A] 20h06
Nst_PDouArgaGois_M150.30_5e-5	Penhas Douradas, Arganil, Góis	Penacova	[B] *	[B] 11h51	[B] *
Nst_PDouArgaPena_M150.30_5e-5	Penhas Douradas, Arganil, Penacova	Góis	[A] *	[B] 11h42	[A/B] *
Nst_PDouGoisPena_M150.30_5e-5	Penhas Douradas, Góis, Penacova	Arganil	[A] 23h14	[A] 9h15	[A] 32h29

* Processing time not present due to interruptions on the simulations.

An overview of *DFreq* and *WSpd* mean errors for each station is presented in Table 10. Additionally, the difference between the errors of the current analysis and the preceding low-altitude stations' analysis, without Penhas Douradas, is presented after each error value. Negative values are considered an improvement. Figure 26, Figure 27, and Figure 28 represent sector-based comparisons charts on the stations of Arganil, Góis, and Penacova, respectively. The top charts represent the *DFreq* (a) and *WSpd* (b) results, and the station's measurements in black. The bottom charts present the *DFreq* (c) and *WSpd* (d) errors. Tables with all the result and error values are present in APPENDIX C. From the examination of the referred figures, the following conclusions were made:

- When compared with the previous low-altitude input stations study, the results of the simulation with the high-altitude Penhas Douradas station as a single input, Nst_PDou_M150.30_5E-5, did not produce more accurate results. The *DFreq* mean errors had the same dimensions as the previous mean, and the *WSpd* mean error increased when compared with the previous better results. The mean *WSpd* increase occurs due to a *WSpd* overestimation in the sectors 210, 240, and 270. This increase can be seen throughout the *WSpd* charts in each station for the mentioned simulation.

- Small improvements when evaluating the results in Góis station were noticed, given that in most cases, the *WSpd* results, that previously were null, were

successfully calculated. On the other hand, when included as an input station, Góis originated *WSpd* results with velocity spikes in sectors 150 and 300. This overestimation harms the results significantly, as most of the mean *WSpd* errors increased when compared with past simulations without Penhas Douradas.

- Similar to the prior sensitivity analysis, the best results originated from the use of Arganil and Penacova as input stations. In these simulations, Nst_PDouArga_M150.30_5e-5 and Nst_PDouArga_M150.30_5e-5, all the errors diminished. The best results were provided by Nst_PDouArga_M150.30_5e-5 to study the location of Penacova, with *DFreq* and *WSpd* mean errors of 2.42 and 22.3%, respectively.
- In general, the simulations' overall results improved when including Penhas Douradas as an input station, with the some previously mentioned exceptions. Through this analysis, an improvement of the results can be expected when including more elevated wind measurements.
- When compared with the previous simulations, the processing time increased considerably, due to the usage of the nesting feature with two simulations and more input stations. Although running these simulations with a single *HighRes* domain would be possible, to include Penhas Douradas station the domain must have the necessary dimensions, as defined for the *LowRes* domain. If the *HighRes* mesh sizes were to be applied onto the *LowRes* domain, the mesh would generate around 8E6 nodes, that, when analysed by the mesh analysis results, would take the undefined 50 plus hours for each input station used.

Table 10 - *DFreq* and *WSpd* mean errors from the simulation with the inclusion of Penhas Douradas station.

Simulation Name	Arganil Station		Góis Station		Penacova Station	
	DFreq Mean Error	WSpd Mean Error [%]	DFreq Mean Error	WSpd Mean Error [%]	DFreq Mean Error	WSpd Mean Error [%]
Nst_PDou_M150.30_5e-5	4.26	86.5	4.83	62.1	2.70	72.1
Nst_PDouArga_M150.30_5e-5	-	-	4.28 (-0.38)	59.2 (-19.5)	2.42 (-1.31)	22.3 (-5.4)
Nst_PDouGois_M300.40_5e-5	4.20 (+0.22)	63.3 (-5.6)	-	-	3.65 (-1.81)	66.1 (-18.8)
Nst_PDouPena_M300.40_5e-5	3.58 (-0.30)	22.6 (-8.0)	5.03 (-0.09)	51.3 (-6.3)	-	-
Nst_PDouArgaGois_M300.40_5e-5	-	-	-	-	3.07 (-1.20)	71.4 (+18.4)
Nst_PDouArgaPena_M300.40_5e-5	-	-	4.68 (+0.38)	53.5 (-7.6)	-	-
Nst_PDouGoisPena_M300.40_5e-5	3.90 (+1.31)	47.0 (+6.5)	-	-	-	-

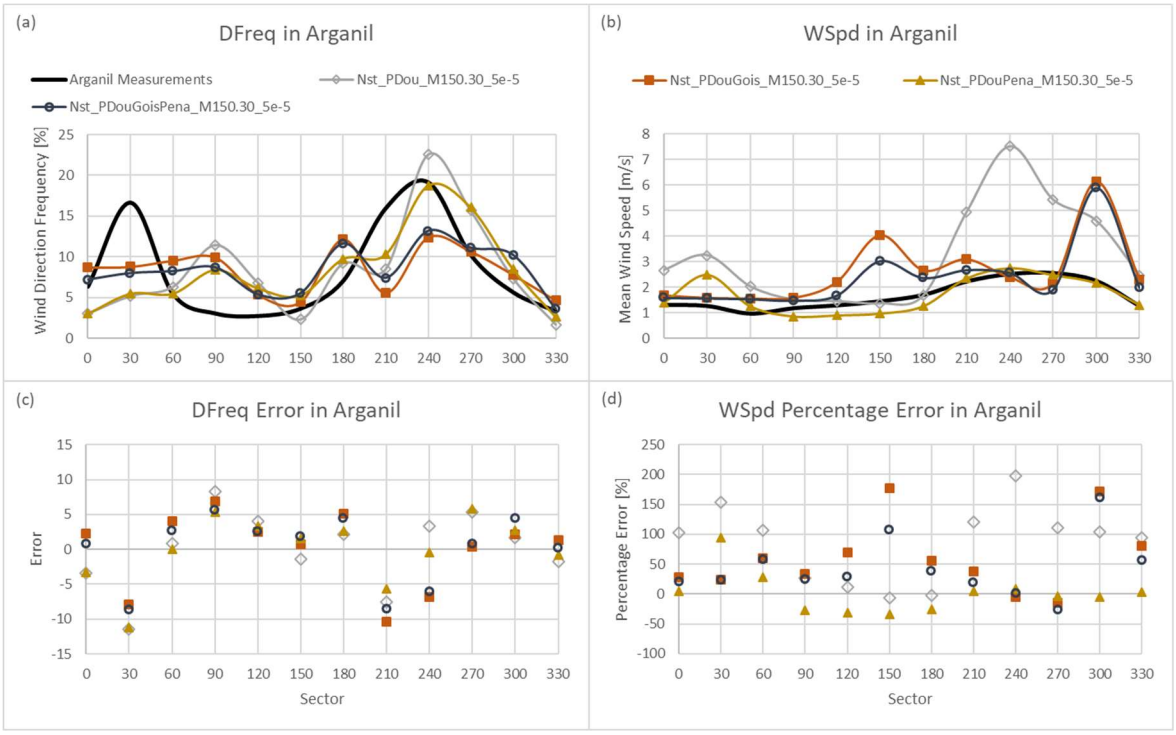

Figure 26 - *DFreq* (a) and *WSpd* (b) results and *DFreq* (c) and *WSpd* (d) error for the inclusion of Penhas Douradas station analysis, in Arganil.

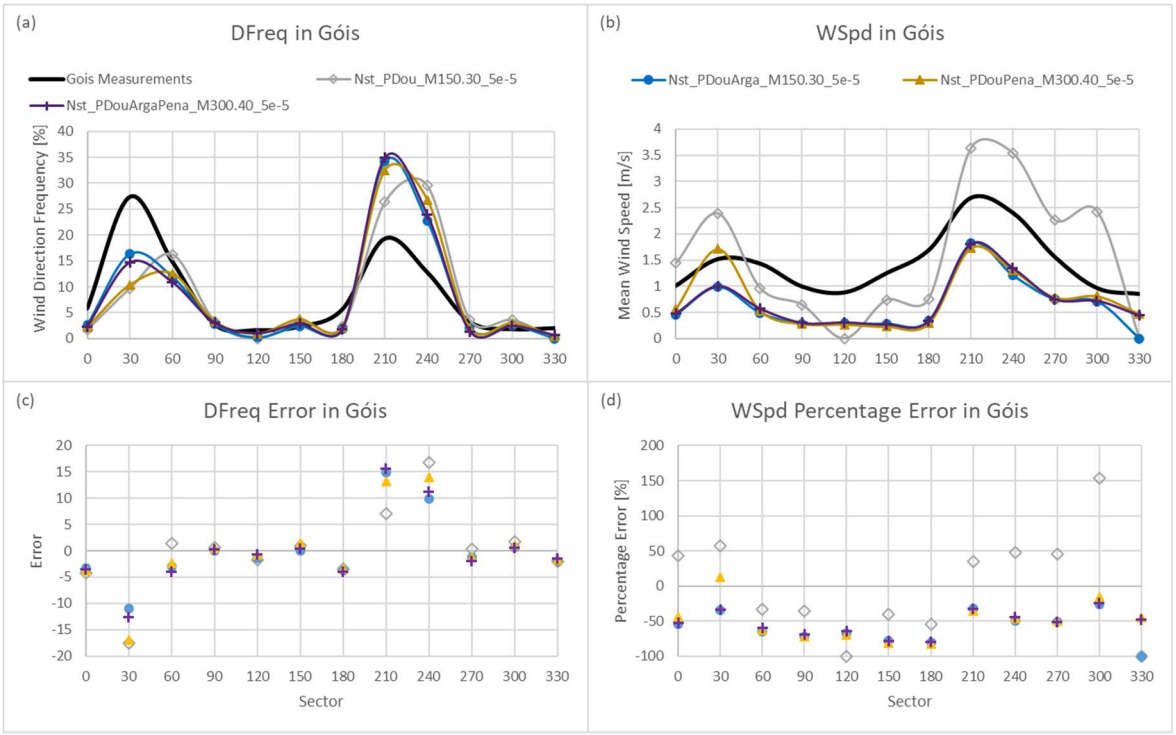

Figure 27 - *DFreq* (a) and *WSpd* (b) results and *DFreq* (c) and *WSpd* (d) errors for the inclusion of Penhas Douradas station analysis, in Góis.

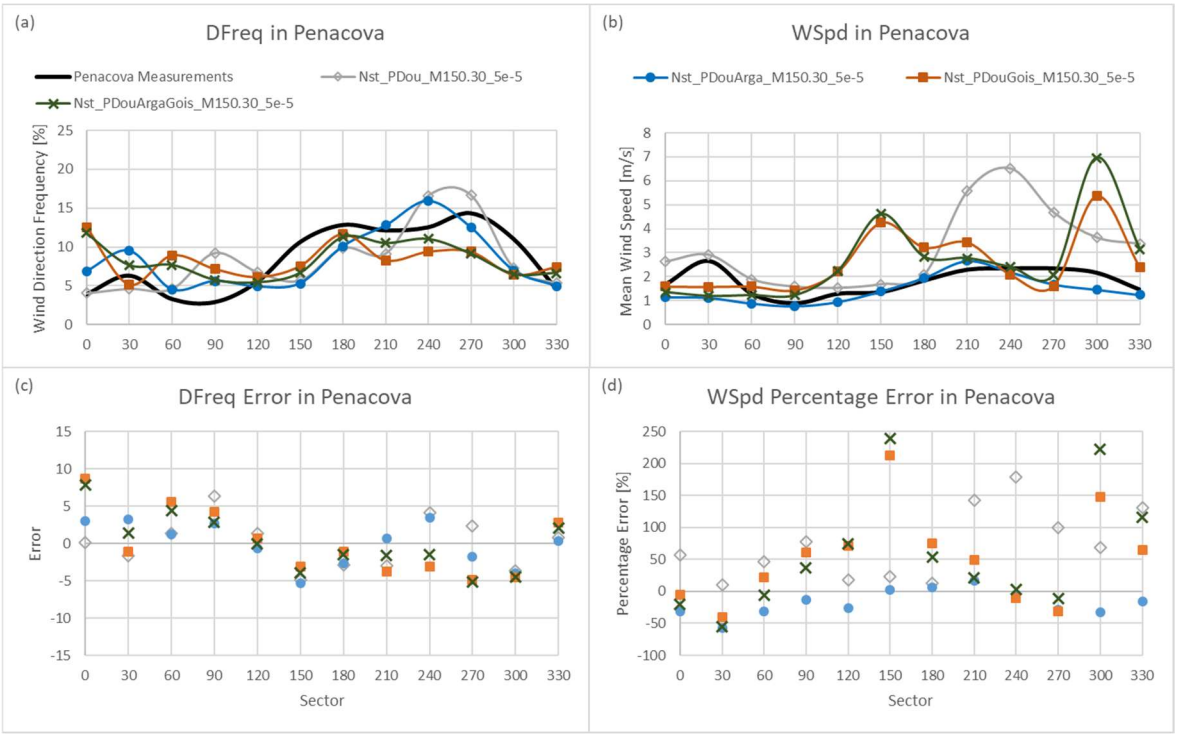

Figure 28 - *DFreq* (a) and *WSpd* (b) results and *DFreq* (c) and *WSpd* (d) errors for the inclusion of Penhas Douradas station analysis, in Penacova.

5. CONCLUSIONS

The present thesis evaluates the performance of the numerical models available in the software WindStation when applied to complex terrain using a climatology approach. For this study, measurements from four meteorological stations in the central region of Portugal were used. In order to evaluate the numeric models, their results were compared with the respective measurements. Two principal situations were studied: a case with three meteorological stations located on small hills and valleys at low altitudes; and a case that included the previous case's stations and included an additional meteorological station located on a mountain. The purpose of these analyses was to verify how the WindStation models would behave with the use of data from various meteorological stations, and with the inclusion of data measured at a higher altitude.

Overall, the simulations were expected to produce better results, as some results, in particular wind sectors, had significant discrepancies when compared with the measured values. The simulations with more input stations did not provide better results, but as expected, the inclusion of measurements from higher altitudes improved the overall outcomes.

From the cases evaluated, a relation between the location of the stations and the simulations results was verified. The station of Góis, situated on a valley, produced poor results when used as an input station. Additionally, due to its location, the simulations in the location of Góis station were challenging, as most of the wind speed results from the valley's side were null. Better results were obtained when using the stations of Arganil and Penacova, for simulating each other's location. The best results were obtained when using the stations of Arganil and Penhas Douradas to study the location of Penacova. Thus, stations with less exposure to the surrounding terrain and measured at higher altitudes, are recommended for the validation of the evaluated model.

Some setbacks were recurrent during the realisation of this thesis. One of the difficulties was the selection of the study location, due to large distances between meteorological stations and lack of measurements in some stations. This factor originated a major setback, which was the inability to optimise the horizontal mesh properly, due to a

large simulation domain. This setback could have been impairing, as it influenced the results significantly, and could have invalidated the remaining of the study. Furthermore, the evaluation of the results was challenging, as the results varied significantly and were unpredictable.

The evaluation of the used models was considered incomplete, meaning that further research is required. In continuation of this study, some other parameters could be evaluated. A possible approach would be to implement obstacles, experiment with the forest model using this study's best-case and test the various turbulence models. Furthermore, to conclude, a more refined mesh should be implemented on the more successful simulations to validate their results.

As a recommendation for following evaluation studies in complex terrains, wind data measured at higher altitudes and with a higher percentage of available data should be used. The area of the study should be smaller, if possible, to allow for a more refined mesh. Furthermore, the definition of obstacles near the measurement station and a forest model could be tested. For the evaluation of the models, besides the assessment with the measurements, an additional comparison with models from similar software packages should be included.

SPECIAL ACKNOWLEDGMENTS

The author wishes to acknowledge IPMA (Instituto Português do Mar e da Atmosfera), for supplying the meteorological source data. Without this collaboration, the present work would not have been possible.

BIBLIOGRAPHY

Berge, E., Gravdahl, A. R., Schelling, J., Tallhaug, L., & Undheim, O. (2006). Wind in complex terrain. A comparison of WAsP and two CFD-models. *European Wind Energy Conference and Exhibition 2006, EWEC 2006*, *2*, 1569–1577.

Cattin, R., Schaffner, B., & Kunz, S. (2006). Validation of CFD wind resource modeling in highly complex terrain. *European Wind Energy Conference and Exhibition 2006, EWEC 2006*, *1*, 36–46.

Djilali, N., Gartshore, I., & Salcudean, M. (1989). Calculation of convective heat transfer in recirculating turbulent flow using various near-wall turbulence models. *Numerical Heat Transfer; Part A: Applications*, *16*(2), 189–212.

Duarte, N. G. L. (2018). Teste de modelos de simulação do campo de ventos para aplicações de avaliação do potencial eólico. In *Dissertação apresentada para a obtenção do grau de Mestre em Engenharia Mecânica na Especialidade de Produção e Projeto*. University of Coimbra.

Giovannini, L., Antonacci, G., Zardi, D., Laiti, L., & Panziera, L. (2014). Sensitivity of simulated wind speed to spatial resolution over complex terrain. *Energy Procedia*, *59*, 323–329.

Jeanmonod, P. J. F. S. (2015). Previsão numérica do vento em torno de topografia complexa- dependência de parâmetros de simulação e comparação com resultados experimentais. In *Dissertação apresentada para a obtenção do grau de Mestre em Engenharia Mecânica na Especialidade de Energia e Ambiente*. University of Coimbra.

Jiménez, P. A., González-Rouco, J. F., Navarro, J., Montávez, J. P., & García-Bustamante, E. (2010). Quality assurance of surface wind observations from automated weather stations. *Journal of Atmospheric and Oceanic Technology*, *27*(7), 1101–1122.

Koblitz, T., Bechmann, A., Sogachev, A., Sørensen, N., & Réthoré, P. E. (2013). Computational fluid dynamics model of stratified atmospheric boundary-layer flow. *Wind Energy*, *18*(1), 75–89.

Launder, B. E., & Spalding, D. B. (1972). Lectures in mathematical models of turbulence. *Academic Press*, 176.

Launder, B. E., & Spalding, D. B. (1974). The numerical computation of turbulent flows. *Computer Methods in Applied Mechanics and Engineering*, *3*(2), 269–289.

Lopes, A. M. G. (2020). *WindStation v1.4.12 - User´s Manual* (v1.4.12). menzio GmbH.

Lopes, A. M. G., Sousa, A. C. M., & Viegas, D. X. (1995). Numerical simulation of turbulent flow and fire propagation in complex topography. *Numerical Heat Transfer, Part A: Applications*, *27*(2), 229–253.

Majumdar, S. (1988). Role of underrelaxation in momentum interpolation for calculation of flow with nonstaggered grids. *Numerical Heat Transfer*, *13*(1), 125–132.

Nielsen, P., Madsen, P., Sørensen, T., Bredelle, K., Sørensen, T., Svenningsen, L., Nielsen, P. M., Funk, R., & Potzka, G. (2020). Energy calculation. In *User guide windPRO 3.4* (p. 213). EMD International A/S.

Nilsson, K. (2010). Estimation of wind energy production in relation to orographic complexity-A reliability study of two conventional computer software. In *Master of Science Thesis*. Chalmers University of Technology.

NOAA SciJinks. (n.d.). *What Is the Coriolis Effect?* Retrieved October 18, 2020, from https://scijinks.gov/coriolis/

Patankar, S. V. (1980). Numerical heat transfer and fluid flow. *Washington, D.C.: Hemisphere Publishing Corporation.*

REN21. (2020). Renewables 2020 Global Status Report. In *REN21 Secretariat*. http://www.ren21.net/resources/publications/

Rhie, C. M., & Chow, W. L. (1983). Numerical study of the turbulent flow past an airfoil with trailing edge separation. *AIAA Journal*, *21*(11), 1525–1532.

Teneler, G. (Högskolan på G. (2011). Wind Flow Analysis on a Complex Terrain: a reliability study of a CFD tool on forested area including effects of forest module. In *Master of Science ThesisWind Power Project Management Spring 2011*. Gotland University.

Theodoropoulos, P., & Deligiorgis, N. (2009). Windsim CFD model validation in a mixed coastal & mountainous region with complex terrain. *European Wind Energy Conference and Exhibition 2009, EWEC 2009*, *6*, 3909–3918.

Thøgersen, M. L., Nielsen, P., Sørensen, T., & Svenningsen, L. U. (2010). An introduction to the MCP facilities in WindPRO. In *EMD International A/S*.

Van Doormaal, J. P., & Raithby, G. D. (1984). Enhancements of the simple method for predicting incompressible fluid flows. *Numerical Heat Transfer*, *7*(2), 147–163.

Wallbank, T. (2008). WindSim Validation Study: CFD validation in Complex terrain. *CFD Validation in Complex Terrain*.

APPENDIX A

Table 11 - Statistical data from the station of Arganil in 2018.

Arganil / Aeródromo (CIM Coimbra) [2018]

Sector		Wind climate				P (1.225)	Quality
#	Angle [°]	Freq. [%]	W-A [m/s]	Weibull-k	U [m/s]	Power [W/m²]	delta-U [%]
1	0	6.4	1.4	1.34	1.32	5	1.01%
2	30	16.7	1.4	1.7	1.28	3	4.72%
3	60	5.5	1.1	1.26	0.98	2	-2.83%
4	90	3.1	1.2	1.02	1.19	6	-4.62%
5	120	2.8	1.3	1.03	1.3	7	-4.34%
6	150	3.7	1.5	1	1.46	11	-2.63%
7	180	7.1	1.8	1.07	1.71	16	-6.45%
8	210	16	2.4	1.34	2.24	23	-2.30%
9	240	19.2	2.8	1.75	2.53	22	0.58%
10	270	10.3	2.9	2.17	2.57	18	3.74%
11	300	5.7	2.5	1.79	2.26	15	3.92%
12	330	3.4	1.4	1.31	1.27	4	0.13%
All (emergent)					1.89	14	

Table 12 - Statistical data from the station of Góis in 2018.

Góis / Quinta da Ribeira (CIM Coimbra) [2018]

Sector		Wind climate				P (1.225)	Quality
#	Angle [°]	Freq. [%]	W-A [m/s]	Weibull-k	U [m/s]	Power [W/m²]	delta-U [%]
1	0	5.9	1.1	1.34	1.01	2	-2.97%
2	30	27.3	1.7	1.92	1.52	4	2.58%
3	60	14.9	1.6	2.27	1.43	3	3.42%
4	90	2.8	1.1	1.5	0.99	2	-1.16%
5	120	1.7	1	1.38	0.88	1	-1.99%
6	150	2.4	1.4	1.89	1.25	2	3.91%
7	180	5.7	1.9	1.77	1.69	6	0.84%
8	210	19.3	3	1.8	2.69	25	-0.25%
9	240	12.8	2.7	2.05	2.4	16	3.26%
10	270	3.3	1.7	1.79	1.55	5	3.16%
11	300	1.9	1	1.31	0.96	2	-4.20%
12	330	2.1	0.9	1.31	0.85	1	-3.13%
All (emergent)					1.77	9	

Table 13 - Statistical data from the station of Penacova in 2018.

Penacova / Hombres (CIM Coimbra) [2018]

Sector		Wind climate				P (1.225)	Quality
#	Angle [°]	Freq. [%]	W-A [m/s]	Weibull-k	U [m/s]	Power [W/m²]	delta-U [%]
1	0	3.9	1.9	1.58	1.68	7	2.16%
2	30	6.3	3	1.59	2.65	29	2.95%
3	60	3.3	1.3	1.14	1.29	6	-1.17%
4	90	2.9	0.9	0.98	0.89	3	-7.16%
5	120	5.5	1.2	0.86	1.29	12	-7.77%
6	150	10.6	1.4	1.1	1.36	7	4.72%
7	180	12.8	1.9	1.11	1.84	18	-6.64%
8	210	12.1	2.5	1.34	2.29	24	0.13%
9	240	12.5	2.6	1.77	2.34	17	2.18%
10	270	14.3	2.6	1.97	2.34	15	1.59%
11	300	11	2.4	1.46	2.16	17	-2.75%
12	330	4.6	1.6	1.65	1.46	5	3.10%
All (emergent)					1.96	15	

Table 14 - Statistical data from the station of Penhas Douradas in 2018.

Penhas Douradas / Observatório (IPMA) [2018]

Sector		Wind climate				P (1.225)	Quality
#	Angle [°]	Freq. [%]	W-A [m/s]	Weibull-k	U [m/s]	Power [W/m²]	delta-U [%]
1	0	2.6	3.2	2.01	2.81	26	0.12%
2	30	2.2	3.2	2.16	2.84	25	2.38%
3	60	2.4	2.7	1.55	2.39	22	0.83%
4	90	6.1	3.1	1.73	2.75	28	-2.43%
5	120	17	3.7	1.86	3.3	45	-2.23%
6	150	11.6	3	1.32	2.81	45	-6.56%
7	180	3.3	2.4	1.09	2.32	38	-9.75%
8	210	2.6	3.5	1.92	3.15	38	0.18%
9	240	6.5	6	2.34	5.27	149	0.49%
10	270	23.2	7.5	2.73	6.69	273	0.38%
11	300	18.3	6.8	1.91	6	264	-2.70%
12	330	4.2	3.9	1.89	3.43	50	0.93%
All (emergent)					4.54	142	

APPENDIX B

Horizontal Mesh Analysis Arganil

Figure 29 - Horizontal mesh analysis in Arganil.

Horizontal Mesh Analysis Góis

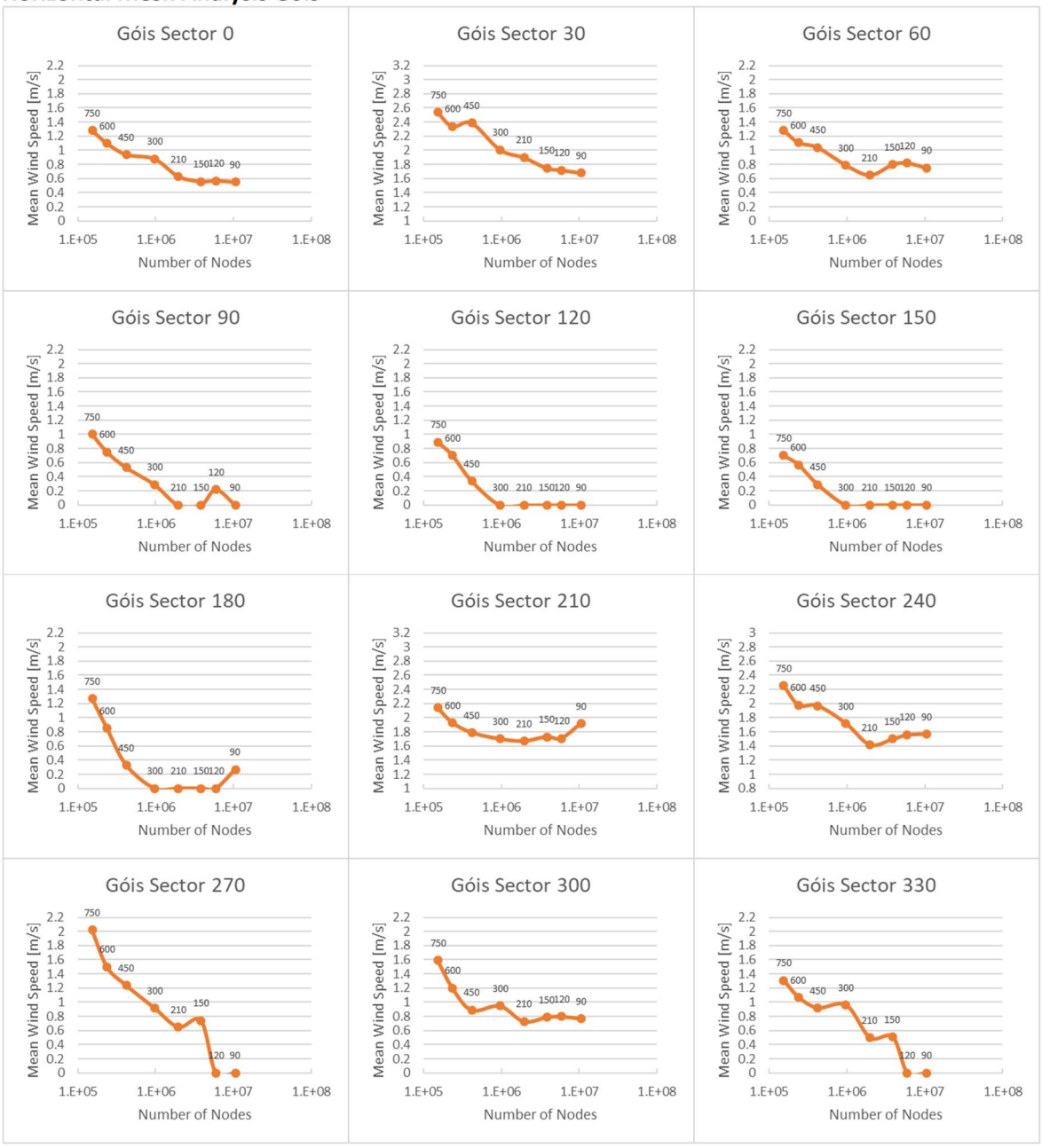

Figure 30 - Horizontal mesh analysis in Góis.

Vertical Mesh Analysis Arganil

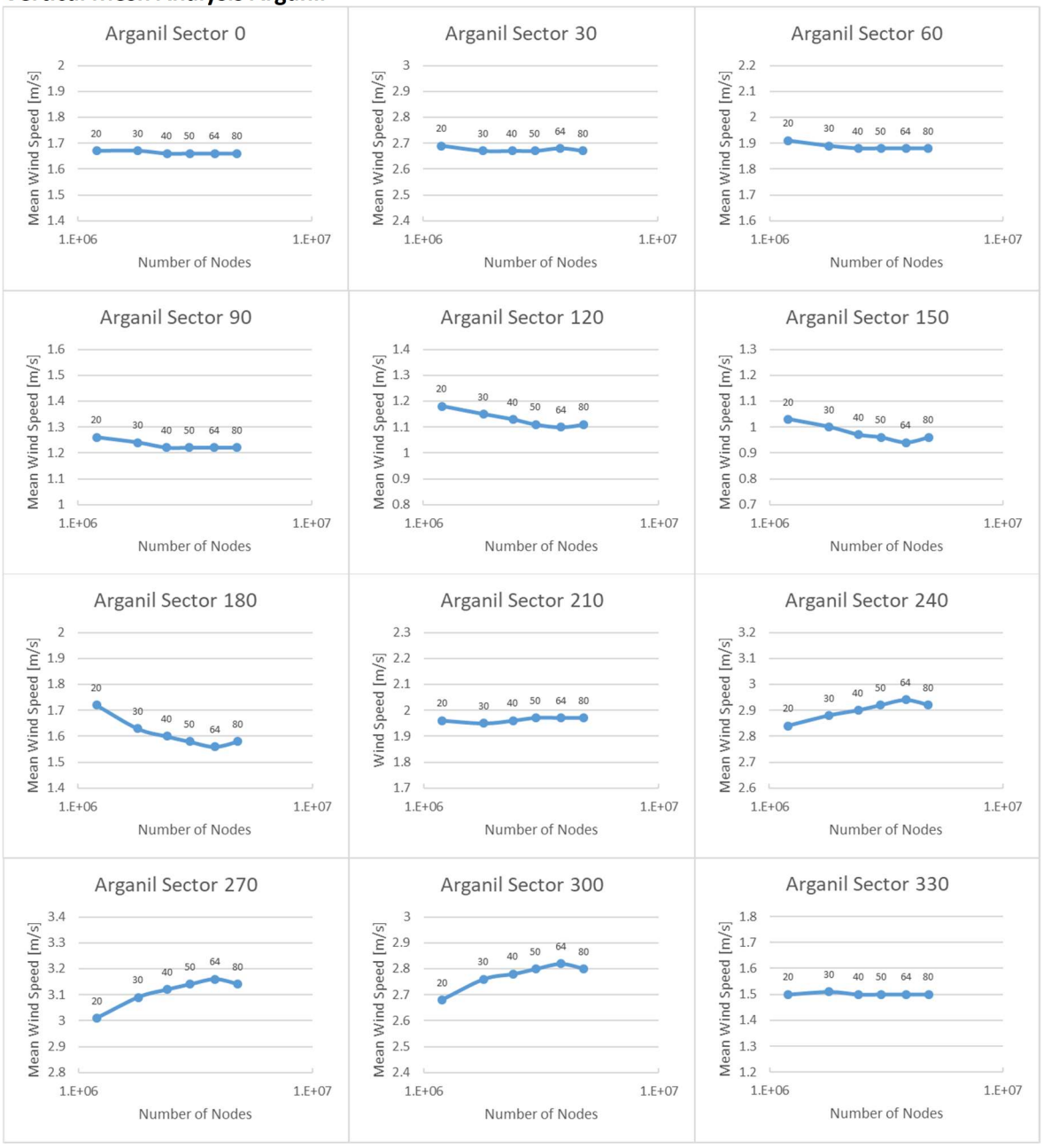

Figure 31 - Vertical mesh analysis in Arganil.

Vertical Mesh Analysis Góis

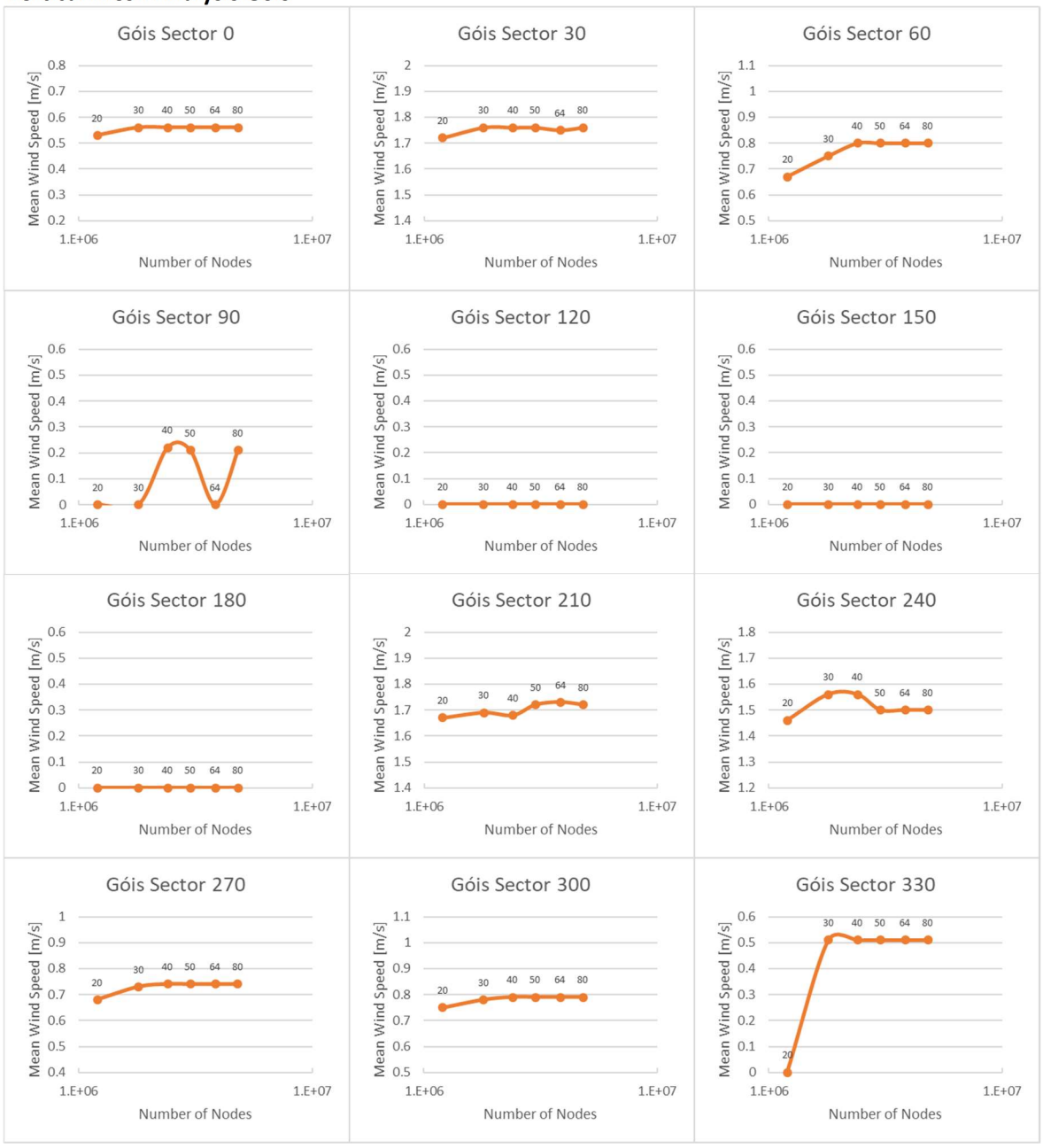

Figure 32 - Vertical mesh analysis in Góis.

APPENDIX C

Table 15 - *DFreq* and *WSpd* results in each sector for the station of Arganil.

Arganil

DFreq [%]													
	Simulation Name	Sector 0	Sector 30	Sector 60	Sector 90	Sector 120	Sector 150	Sector 180	Sector 210	Sector 240	Sector 270	Sector 300	Sector 330	Mean
	Measurements	6.40	16.70	5.50	3.10	2.80	3.70	7.10	16.00	19.20	10.30	5.70	3.40	-------
Input Stations	Gois_M150.30_5e-5	12.72	16.46	8.49	6.00	8.72	0.66	10.57	13.96	6.42	7.67	2.56	5.76	-------
	Pena_M150.30_5e-5	3.09	5.77	4.57	5.09	7.58	6.44	10.27	12.26	14.88	16.51	9.80	3.73	-------
	GoisPena_M150.30_5e-5	6.56	11.98	8.59	5.59	6.71	4.87	4.97	12.52	14.15	13.22	5.58	5.26	-------
Penhas Douradas	Nst_PDou_M150.30_5e-5	3.02	5.19	6.31	11.45	6.82	2.30	9.19	8.48	22.56	15.66	7.34	1.67	-------
	Nst_PDouGois_M150.30_5e-5	8.70	8.78	9.53	9.92	5.36	4.48	12.15	5.58	12.38	10.66	7.80	4.67	-------
	Nst_PDouPena_M150.30_5e-5	3.05	5.50	5.52	8.43	6.15	5.28	9.77	10.32	18.78	16.08	8.48	2.63	-------
	Nst_PDouGoisPena_M150.30_5e-5	7.19	7.98	8.22	8.68	5.36	5.52	11.61	7.40	13.17	11.10	10.20	3.57	-------
WSpd [m/s]														
	Simulation Name	Sector 0	Sector 30	Sector 60	Sector 90	Sector 120	Sector 150	Sector 180	Sector 210	Sector 240	Sector 270	Sector 300	Sector 330	Mean
	Measurements	1.32	1.28	0.98	1.19	1.30	1.46	1.71	2.24	2.53	2.57	2.26	1.27	**1.89**
Input Stations	Gois_M150.30_5e-5	1.64	1.64	1.92	2.18	4.56	2.56	2.40	2.80	3.48	3.72	3.49	2.12	**2.55**
	Pena_M150.30_5e-5	1.67	2.67	1.89	1.24	1.15	1.00	1.63	1.95	2.88	3.09	2.76	1.51	**2.18**
	GoisPena_M150.30_5e-5	1.54	1.66	1.87	1.94	2.34	2.46	1.86	2.82	3.15	2.92	1.87	1.87	**2.33**
Penhas Douradas	Nst_PDou_M150.30_5e-5	2.67	3.25	2.03	1.51	1.45	1.36	1.67	4.94	7.52	5.43	4.60	2.47	**4.18**
	Nst_PDouGois_M150.30_5e-5	1.69	1.59	1.57	1.59	2.21	4.04	2.67	3.10	2.40	2.18	6.13	2.30	**2.50**
	Nst_PDouPena_M150.30_5e-5	1.39	2.49	1.26	0.86	0.90	0.97	1.26	2.35	2.75	2.48	2.16	1.31	**1.93**
	Nst_PDouGoisPena_M150.30_5e-5	1.59	1.57	1.54	1.48	1.68	3.03	2.37	2.68	2.57	1.91	5.90	1.98	**2.45**

Table 16 - *DFreq* and *WSpd* errors in each sector for the station of Arganil.

Arganil

DFreq Error													
	Simulation Name	Sector 0	Sector 30	Sector 60	Sector 90	Sector 120	Sector 150	Sector 180	Sector 210	Sector 240	Sector 270	Sector 300	Sector 330	Mean
Input Stations	Gois_M150.30_5e-5	6.32	-0.24	2.99	2.90	5.92	-3.04	3.47	-2.04	-12.78	-2.63	-3.14	2.36	**3.99**
	Pena_M150.30_5e-5	-3.31	-10.93	-0.93	1.99	4.78	2.74	3.17	-3.74	-4.32	6.21	4.10	0.33	**3.88**
	GoisPena_M150.30_5e-5	0.16	-4.72	3.09	2.49	3.91	1.17	-2.13	-3.48	-5.05	2.92	-0.12	1.86	**2.59**
Penhas Douradas	Nst_PDou_M150.30_5e-5	-3.38	-11.51	0.81	8.35	4.02	-1.40	2.09	-7.52	3.36	5.36	1.64	-1.73	**4.26**
	Nst_PDouGois_M150.30_5e-5	2.30	-7.92	4.03	6.82	2.56	0.78	5.05	-10.42	-6.82	0.36	2.10	1.27	**4.20**
	Nst_PDouPena_M150.30_5e-5	-3.35	-11.20	0.02	5.33	3.35	1.58	2.67	-5.68	-0.42	5.78	2.78	-0.77	**3.58**
	Nst_PDouGoIsPena_M150.30_5e-5	0.79	-8.72	2.72	5.58	2.56	1.82	4.51	-8.60	-6.03	0.80	4.50	0.17	**3.90**
WSpd Error [%]														
	Simulation Name	Sector 0	Sector 30	Sector 60	Sector 90	Sector 120	Sector 150	Sector 180	Sector 210	Sector 240	Sector 270	Sector 300	Sector 330	Mean
Input Stations	Gois_M150.30_5e-5	24.2	28.1	95.9	83.2	250.8	75.3	40.4	25.0	37.5	44.7	54.4	66.9	**68.9**
	Pena_M150.30_5e-5	26.5	108.6	92.9	4.2	-11.5	-31.5	-4.7	-12.9	13.8	20.2	22.1	18.9	**30.7**
	GoisPena_M150.30_5e-5	16.7	29.7	90.8	63.0	80.0	68.5	8.8	25.9	24.5	13.6	-17.3	47.2	**40.5**
Penhas Douradas	Nst_PDou_M150.30_5e-5	102.3	153.9	107.1	26.9	11.5	-6.8	-2.3	120.5	197.2	111.3	103.5	94.5	**86.5**
	Nst_PDouGois_M150.30_5e-5	28.0	24.2	60.2	33.6	70.0	176.7	56.1	38.4	-5.1	-15.2	171.2	81.1	**63.3**
	Nst_PDouPena_M150.30_5e-5	5.3	94.5	28.6	-27.7	-30.8	-33.6	-26.3	4.9	8.7	-3.5	-4.4	3.1	**22.6**
	Nst_PDouGoisPena_M150.30_5e-5	20.5	22.7	57.1	24.4	29.2	107.5	38.6	19.6	1.6	-25.7	161.1	55.9	**47.0**

Table 17 - *DFreq* and *WSpd* results in each sector for the station of Góis.

Góis

DFreq [%]													
	Simulation Name	Sector 0	Sector 30	Sector 60	Sector 90	Sector 120	Sector 150	Sector 180	Sector 210	Sector 240	Sector 270	Sector 300	Sector 330	Mean
	Measurements	5.90	27.30	14.90	2.80	1.70	2.40	5.70	19.30	12.80	3.30	1.90	2.10	-------
Input Stations	Arga_M150.30_5e-5	3.17	26.61	7.40	1.10	0.55	0.00	0.00	40.91	19.13	0.00	0.00	1.14	-------
	Pena_M150.30_5e-5	1.85	12.01	9.57	4.33	2.13	2.13	2.13	37.10	23.42	2.21	2.21	0.92	-------
	ArgaPena_M150.30_5e-5	1.94	19.03	8.00	3.03	1.63	1.46	1.81	38.59	19.00	2.79	1.69	1.03	-------
Penhas Douradas	Nst_PDou_M150.30_5e-5	1.67	9.70	16.29	3.40	0.00	3.40	2.31	26.34	29.58	3.66	3.66	0.00	-------
	Nst_PDouArga_M150.30_5e-5	2.62	16.33	11.98	2.87	0.24	2.44	1.94	34.23	22.73	2.06	2.56	0.00	-------
	Nst_PDouPena_M300.40_5e-5	2.18	10.32	12.55	3.32	0.97	3.76	2.23	32.43	26.79	2.00	3.01	0.42	-------
	Nst_PDouArgaPena_M300.40_5e-5	2.36	14.69	10.92	3.03	1.02	2.86	1.78	34.92	23.96	1.39	2.44	0.64	-------
WSpd [m/s]														
	Simulation Name	Sector 0	Sector 30	Sector 60	Sector 90	Sector 120	Sector 150	Sector 180	Sector 210	Sector 240	Sector 270	Sector 300	Sector 330	Mean
	Measurements	1.01	1.52	1.43	0.99	0.88	1.25	1.69	2.69	2.40	1.55	0.96	0.85	**1.77**
Input Stations	Arga_M150.30_5e-5	0.43	0.93	0.60	0.00	0.00	0.00	0.00	1.65	1.14	0.00	0.00	0.00	**1.20**
	Pena_M150.30_5e-5	0.56	1.76	0.75	0.00	0.00	0.00	0.00	1.69	1.56	0.73	0.78	0.51	**1.32**
	ArgaPena_M150.30_5e-5	0.46	0.95	0.68	0.00	0.00	0.00	0.28	1.69	1.61	0.60	0.65	0.50	**1.24**
Penhas Douradas	Nst_PDou_M150.30_5e-5	1.44	2.39	0.96	0.64	0.00	0.74	0.76	3.64	3.54	2.26	2.43	0.00	**2.66**
	Nst_PDouArga_M150.30_5e-5	0.46	0.99	0.49	0.28	0.29	0.28	0.34	1.82	1.21	0.75	0.71	0.00	**1.19**
	Nst_PDouPena_M300.40_5e-5	0.57	1.71	0.53	0.28	0.27	0.23	0.29	1.73	1.30	0.78	0.81	0.47	**1.23**
	Nst_PDouArgaPena_M300.40_5e-5	0.48	1.00	0.57	0.30	0.31	0.27	0.34	1.80	1.34	0.75	0.72	0.44	**1.23**

Table 18 - *DFreq* and *WSpd* errors in each sector for the station of Góis.

Góis

DFreq Error													
	Simulation Name	Sector 0	Sector 30	Sector 60	Sector 90	Sector 120	Sector 150	Sector 180	Sector 210	Sector 240	Sector 270	Sector 300	Sector 330	Mean
Input Stations	Arga_M150.30_5e-5	-2.73	-0.69	-7.50	-1.70	-1.15	-2.40	-5.70	21.61	6.33	-3.30	-1.90	-0.96	**4.66**
	Pena_M150.30_5e-5	-4.05	-15.29	-5.33	1.53	0.43	-0.27	-3.57	17.80	10.62	-1.09	0.31	-1.18	**5.12**
	ArgaPena_M150.30_5e-5	-3.96	-8.27	-6.90	0.23	-0.07	-0.94	-3.89	19.29	6.20	-0.51	-0.21	-1.07	**4.30**
Penhas Douradas	Nst_PDou_M150.30_5e-5	-4.23	-17.60	1.39	0.60	-1.70	1.00	-3.39	7.04	16.78	0.36	1.76	-2.10	**4.83**
	Nst_PDouArga_M150.30_5e-5	-3.28	-10.97	-2.92	0.07	-1.46	0.04	-3.76	14.93	9.93	-1.24	0.66	-2.10	**4.28**
	Nst_PDouPena_M300.40_5e-5	-3.72	-16.98	-2.35	0.52	-0.73	1.36	-3.47	13.13	13.99	-1.30	1.11	-1.68	**5.03**
	Nst_PDouArgaPena_M300.40_5e-5	-3.54	-12.61	-3.98	0.23	-0.68	0.46	-3.92	15.62	11.16	-1.91	0.54	-1.46	**4.68**
WSpd Error [%]														
	Simulation Name	Sector 0	Sector 30	Sector 60	Sector 90	Sector 120	Sector 150	Sector 180	Sector 210	Sector 240	Sector 270	Sector 300	Sector 330	Mean
Input Stations	Arga_M150.30_5e-5	-57.4	-38.8	-58.0	-100.0	-100.0	-100.0	-100.0	-38.7	-52.5	-100.0	-100.0	-100.0	**78.8**
	Pena_M150.30_5e-5	-44.6	15.8	-47.6	-100.0	-100.0	-100.0	-100.0	-37.2	-35.0	-52.9	-18.8	-40.0	**57.6**
	ArgaPena_M150.30_5e-5	-54.5	-37.5	-52.4	-100.0	-100.0	-100.0	-83.4	-37.2	-32.9	-61.3	-32.3	-41.2	**61.1**
Penhas Douradas	Nst_PDou_M150.30_5e-5	42.6	57.2	-32.9	-35.4	-100.0	-40.8	-55.0	35.3	47.5	45.8	153.1	-100.0	**62.1**
	Nst_PDouArga_M150.30_5e-5	-54.5	-34.9	-65.7	-71.7	-67.0	-77.6	-79.9	-32.3	-49.6	-51.6	-26.0	-100.0	**59.2**
	Nst_PDouPena_M300.40_5e-5	-43.6	12.5	-62.9	-71.7	-69.3	-81.6	-82.8	-35.7	-45.8	-49.7	-15.6	-44.7	**51.3**
	Nst_PDouArgaPena_M300.40_5e-5	-52.5	-34.2	-60.1	-69.7	-64.8	-78.4	-79.9	-33.1	-44.2	-51.6	-25.0	-48.2	**53.5**

Table 19 - *DFreq* and *WSpd* results in each sector for the station of Penacova.

Penacova

DFreq [%]													
	Simulation Name	Sector 0	Sector 30	Sector 60	Sector 90	Sector 120	Sector 150	Sector 180	Sector 210	Sector 240	Sector 270	Sector 300	Sector 330	Mean
	Measurements	3.90	6.30	3.30	2.90	5.50	10.60	12.80	12.10	12.50	14.30	11.00	4.60	-------
Input Stations	Arga_M150.30_5e-5	9.80	14.57	4.45	2.52	2.32	4.90	10.32	16.54	15.20	8.21	6.59	4.59	-------
	Gois_M150.30_5e-5	18.20	10.90	8.42	5.94	6.49	2.86	15.41	13.07	2.58	5.15	5.15	5.82	-------
	ArgaGois_M150.30_5e-5	14.76	12.39	6.78	4.53	4.78	3.70	13.32	14.48	7.75	6.41	5.74	5.34	-------
Penhas Douradas	Nst_PDou_M150.30_5e-5	4.05	4.64	4.61	9.23	6.80	5.70	9.87	9.15	16.60	16.67	7.34	5.34	-------
	Nst_PDouArga_M150.30_5e-5	6.87	9.52	4.53	5.60	4.89	5.30	10.09	12.79	15.96	12.53	6.97	4.96	-------
	Nst_PDouGois_M150.30_5e-5	12.56	5.17	8.91	7.18	6.13	7.53	11.66	8.28	9.38	9.37	6.43	7.40	-------
	Nst_PDouArgaGois_M150.30_5e-5	11.78	7.65	7.68	5.75	5.42	6.65	11.28	10.50	11.03	9.13	6.50	6.64	-------
WSpd [m/s]														
	Simulation Name	Sector 0	Sector 30	Sector 60	Sector 90	Sector 120	Sector 150	Sector 180	Sector 210	Sector 240	Sector 270	Sector 300	Sector 330	Mean
	Measurements	1.68	2.65	1.29	0.89	1.29	1.36	1.84	2.29	2.34	2.34	2.16	1.46	**1.96**
Input Stations	Arga_M150.30_5e-5	1.18	1.03	0.85	1.16	1.33	2.00	2.57	2.36	1.80	1.75	1.67	1.27	**1.70**
	Gois_M150.30_5e-5	1.57	1.56	1.85	2.12	4.68	5.50	3.27	3.27	2.91	2.81	2.76	1.90	**2.60**
	ArgaGois_M150.30_5e-5	1.58	1.16	1.29	1.42	3.14	4.32	2.94	2.65	2.13	2.36	2.40	2.29	**2.19**
Penhas Douradas	Nst_PDou_M150.30_5e-5	2.63	2.91	1.89	1.58	1.53	1.68	2.08	5.56	6.51	4.68	3.63	3.37	**3.70**
	Nst_PDouArga_M150.30_5e-5	1.15	1.12	0.88	0.77	0.95	1.39	1.95	2.66	2.19	1.68	1.46	1.24	**1.65**
	Nst_PDouGois_M150.30_5e-5	1.58	1.57	1.58	1.43	2.21	4.25	3.22	3.43	2.08	1.61	5.36	2.40	**2.51**
	Nst_PDouArgaGois_M150.30_5e-5	1.35	1.19	1.22	1.22	2.25	4.61	2.82	2.77	2.40	2.08	6.96	3.15	**2.57**

Table 20 - *DFreq* and *WSpd* errors in each sector for the station of Penacova.

Penacova

DFreq Error													
	Simulation Name	Sector 0	Sector 30	Sector 60	Sector 90	Sector 120	Sector 150	Sector 180	Sector 210	Sector 240	Sector 270	Sector 300	Sector 330	Mean
Input Stations	Arga_M150.30_5e-5	5.90	8.27	1.15	-0.38	-3.18	-5.70	-2.48	4.44	2.70	-6.09	-4.41	-0.01	**3.73**
	Gois_M150.30_5e-5	14.30	4.60	5.12	3.04	0.99	-7.74	2.61	0.97	-9.92	-9.15	-5.85	1.22	**5.46**
	ArgaGois_M150.30_5e-5	10.86	6.09	3.48	1.63	-0.72	-6.90	0.52	2.38	-4.75	-7.89	-5.26	0.74	**4.27**
Penhas Douradas	Nst_PDou_M150.30_5e-5	0.15	-1.66	1.31	6.33	1.30	-4.90	-2.93	-2.95	4.10	2.37	-3.66	0.74	**2.70**
	Nst_PDouArga_M150.30_5e-5	2.97	3.22	1.23	2.70	-0.61	-5.30	-2.71	0.69	3.46	-1.77	-4.03	0.36	**2.42**
	Nst_PDouGois_M150.30_5e-5	8.66	-1.13	5.61	4.28	0.63	-3.07	-1.14	-3.82	-3.12	-4.93	-4.57	2.80	**3.65**
	Nst_PDouArgaGois_M150.30_5e-5	7.88	1.35	4.38	2.85	-0.08	-3.95	-1.52	-1.60	-1.47	-5.17	-4.50	2.04	**3.07**
WSpd Error [%]														
	Simulation Name	Sector 0	Sector 30	Sector 60	Sector 90	Sector 120	Sector 150	Sector 180	Sector 210	Sector 240	Sector 270	Sector 300	Sector 330	Mean
Input Stations	Arga_M150.30_5e-5	-29.8	-61.1	-34.1	30.3	3.1	47.1	39.7	3.1	-23.1	-25.2	-22.7	-13.0	**27.7**
	Gois_M150.30_5e-5	-6.5	-41.1	43.4	138.2	262.8	304.4	77.7	42.8	24.4	20.1	27.8	30.1	**84.9**
	ArgaGois_M150.30_5e-5	-6.0	-56.2	0.0	59.6	143.4	217.6	59.8	15.7	-9.0	0.9	11.1	56.8	**53.0**
Penhas Douradas	Nst_PDou_M150.30_5e-5	56.5	9.8	46.5	77.5	18.6	23.5	13.0	142.8	178.2	100.0	68.1	130.8	**72.1**
	Nst_PDouArga_M150.30_5e-5	-31.5	-57.7	-31.8	-13.5	-26.4	2.2	6.0	16.2	-6.4	-28.2	-32.4	-15.1	**22.3**
	Nst_PDouGois_M150.30_5e-5	-6.0	-40.8	22.5	60.7	71.3	212.5	75.0	49.8	-11.1	-31.2	148.1	64.4	**66.1**
	Nst_PDouArgaGois_M150.30_5e-5	-19.6	-55.1	-5.4	37.1	74.4	239.0	53.3	21.0	2.6	-11.1	222.2	115.8	**71.4**